M. Hamed Mohammady | Alexia Auffèves | Janet Anders

Energetic footprints of irreversibility in the quantum regime

Journal article | Version of record

ARTICLE

Check for updates

Energetic footprints of irreversibility in the quantum regime

M. H. Mohammady[1,2,3 ✉], A. Auffèves[4 ✉] & J. Anders[1,5 ✉]

In classical thermodynamic processes the unavoidable presence of irreversibility, quantified by the entropy production, carries two energetic footprints: the reduction of extractable work from the optimal, reversible case, and the generation of a surplus of heat that is irreversibly dissipated to the environment. Recently it has been shown that in the quantum regime an additional quantum irreversibility occurs that is linked to decoherence into the energy basis. Here we employ quantum trajectories to construct distributions for classical heat and quantum heat exchanges, and show that the heat footprint of quantum irreversibility differs markedly from the classical case. We also quantify how quantum irreversibility reduces the amount of work that can be extracted from a state with coherences. Our results show that decoherence leads to both entropic and energetic footprints which both play an important role in the optimization of controlled quantum operations at low temperature.

[1] CEMPS, Physics and Astronomy, University of Exeter, Exeter EX4 4QL, UK. [2] Department of Physics, Lancaster University, Lancaster LA1 4YB, UK. [3] RCQI, Institute of Physics, Slovak Academy of Sciences, Dúbravská cesta 9, 84511 Bratislava, Slovakia. [4] CNRS and Université Grenoble Alpes, Institut Néel, F-38042 Grenoble, France. [5] Institute of Physics and Astronomy, University of Potsdam, 14476 Potsdam, Germany. ✉email: m.hamed.mohammady@savba.sk; alexia.auffeves@neel.cnrs.fr; janet@qipc.org

In recent years much effort has been made in extending the laws of thermodynamics to the quantum regime[1–4]. Maximal work extraction (or minimal work cost) has been discussed for a range of protocols[5–24], showing that energetic coherences can be a resource for work extraction[25–29] while quantum correlations can reduce the work cost of erasing information[30]. However, many of these studies have focussed on the optimal limit of reversible processes, i.e., unitary and quasi-static evolutions, without discussing the limitations that irreversibility puts on work extraction. On the other hand, the irreversibility of thermodynamic processes in the quantum regime has been explored using stochastic thermodynamics[31–39] leading to the notion of a fluctuating quantum entropy production[40] that obeys a fluctuation theorem analogous to those of classical nonequilibrium dynamics[41–43]. First experiments have now measured entropy production rates in driven mesoscopic quantum systems for two platforms, a micromechanical resonator and a Bose–Einstein condensate[44]. Most recently, the average entropy production of a quantum system that interacts with another (non-bath) system, has been shown to include an additional information flow term[45].

In classical thermodynamics irreversibility occurs whenever a nonthermal system is brought into contact with a thermal environment. The ensuing relaxation of the system leads to exchanges of energy that cannot be reversed with the same thermodynamic cost. In thermodynamics this irreversibility is quantified by the positive "irreversible entropy production" $S_{\text{irr}} := \Delta S - \frac{Q}{T} \geq 0$, which measures the discrepancy between the system's entropy increase $\Delta S = S_{\text{fin}} - S_{\text{ini}}$ during any thermodynamic process and the heat Q absorbed by the system from the environment divided by the environment's temperature T. Hence when a process with entropy change ΔS incurs a non-zero entropy production S_{irr} this results in a surplus of heat[46],

$$Q_{\text{diss}}^{\text{sur}} = T\, S_{\text{irr}}, \tag{1}$$

that is irreversibly dissipated from the system to the environment (in comparison with a reversible process resulting in the same entropy change ΔS). Irreversibility also puts a fundamental bound on the amount of work W_{ext} that can be extracted during isothermal processes[46,47],

$$W_{\text{ext}} = -\Delta F - T S_{\text{irr}} \leq -\Delta F, \tag{2}$$

where $\Delta F = F_{\text{fin}} - F_{\text{ini}}$ is the system's free energy increase. The more irreversible a process is, the less work can be extracted and the term $W_{\text{irr}} = T S_{\text{irr}}$ may be called the irreversible work, or non-recoverable work[48]. Eqs. (1) and (2) link entropy production, S_{irr} to a surplus in heat dissipation, $Q_{\text{diss}}^{\text{sur}} \geq 0$, and a reduction in work extraction, $W_{\text{ext}} \leq -\Delta F$. These relationships are the well-known energetic footprints of irreversibility in classical thermodynamics.

A quantum system can be out of equilibrium in two ways: by maintaining energetic probabilities that are nonthermal, and by maintaining coherences between energy levels. It has been shown that contact with the thermal environment gives rise to a classical and a quantum aspect of irreversibility[34,35]. Moreover, in addition to the exchange of energy quanta between the quantum system and the thermal environment—known as classical heat—whenever the system has "energy coherence" it will exhibit a uniquely quantum energy exchange known as "quantum heat"[23,33,36,37,49,50]. However, thus far the link between quantum entropy production and its energetic footprints has remained opaque.

In this paper we establish the energetic footprints of irreversibility in the quantum regime, arising whenever a system is brought in contact with a thermal environment. For concreteness, we here consider a specific protocol that extracts work from a quantum system's coherences in the energy basis[27]. We first extend the protocol to capture irreversible steps that are unavoidable in any experimental implementation and which will affect heat and work exchanges. By employing the eigenstate trajectory unraveling of the open system dynamics, where at the start and end of each dynamical process the system is assumed to be in one of the eigenstates of its time-local density matrix, we identify the distributions of classical and quantum heat, and evidence that purely quantum contributions to the entropy production are not related to the average quantum heat, in stark contrast to the classical regime, cf. Eq. (1). Instead, we show that the average quantum entropy production, $\langle s_{\text{irr}}^{\text{qu}} \rangle$, is linked with the variance in quantum heat, $\text{Var}(Q_{\text{qu}})$, a quantity that has recently been connected to entanglement generation[51]. Specifically, we show that $\langle s_{\text{irr}}^{\text{qu}} \rangle = 0$ if and only if $\text{Var}(Q_{\text{qu}}) = 0$, while both $\langle s_{\text{irr}}^{\text{qu}} \rangle$ and the lower bounds to $\text{Var}(Q_{\text{qu}})$ monotonically decrease under Hamiltonian-covariant channels. In the special case of qubits, this relationship becomes stronger, and we show that: (i) for the family of states ρ with the same spectrum, but different eigenbases, $\langle s_{\text{irr}}^{\text{qu}} \rangle$ and $\text{Var}(Q_{\text{qu}})$ are co-monotonic with the energy coherence of the eigenbasis of ρ; and (ii) both $\langle s_{\text{irr}}^{\text{qu}} \rangle$ and $\text{Var}(Q_{\text{qu}})$ monotonically decrease under the action of Hamiltonian-covariant channels that are a combination of dephasing and depolarization. Both of these strong monotonicity relationships break down for systems with a larger Hilbert space, which we illustrate with a simple example for a three-level system. We also note that no such relationship exists between the average classical entropy production $\langle s_{\text{irr}}^{\text{cl}} \rangle$ and the variance in classical heat $\text{Var}(Q_{\text{cl}})$; even in the case of qubits one does not monotonically increase with the other, and furthermore $\langle s_{\text{irr}}^{\text{cl}} \rangle = 0$ is neither necessary nor sufficient for $\text{Var}(Q_{\text{cl}}) = 0$, with the latter condition only being achieved in the limit of zero temperature. Finally, we show that the classical and quantum entropy production reduce the extractable work from coherence in equal measure, cf. Eq. (2). The results show that when experimental imperfections are unavoidable, any work-optimization strategy needs to consider the trade-off between a system having a certain degree of classical non-thermality or quantum coherence, or both. Besides being of fundamental importance for the development of a general quantum thermodynamics framework that includes irreversibility, these relations will also be crucial for the assessment of the energetic cost of quantum control protocols, that aim to optimize performance of computation and communication in the presence of decoherence and noise.

Results

Imperfect protocol for work extraction from coherences. We here outline the protocol for optimal work extraction from coherences introduced in ref. [27], and modify it so as to include imperfections that result in both classical and quantum irreversibility. This protocol can be implemented for any d-dimensional system, but we shall pay special interest to the qubit case for illustrative purposes. For a d-dimensional quantum system with Hamiltonian H and quantum state ρ we denote by (ρ, H) any nonequilibrium configuration of the system, and by $(\tau, H)_T$ with $\tau := e^{-H/(k_B T)}/Z$ and partition function $Z := \text{tr}[e^{-H/(k_B T)}]$ its equilibrium configuration at temperature T[52]. The protocol will involve quenching of the system Hamiltonian in N discrete steps, denoted $H^{(0)} \mapsto H^{(1)} \mapsto \cdots \mapsto H^{(N)}$. Moreover, $H^{(j)}$ for $j = 0, 1, \ldots, N$ are chosen diagonal in the same basis, i.e., only the spectrum of the Hamiltonian varies during the protocol. Specifically, $H^{(j)} := \sum_{k=1}^{d} E_k^{(j)} \Pi[e_k]$, where $E_k^{(j)}$ are energy eigenvalues, and $\Pi[\psi] \equiv |\psi\rangle\langle\psi|$ denotes the projection onto the pure state $|\psi\rangle$. The system is initially prepared in an arbitrary mixed state

$$\rho := \sum_{l=1}^{d} p_l\, \Pi[\psi_l], \tag{3}$$

with $p_l > 0$ for all l, $\sum_l p_l = 1$, and $\{\lvert\psi_l\rangle\}$ an arbitrary orthonormal basis.

The protocol transfers ρ to the fixed final state η chosen to have the same energetic probabilities as the initial state ρ but with the energetic coherences removed[27], i.e., the system's final state is

$$\eta := \sum_k \Pi[e_k]\, \rho\, \Pi[e_k] \equiv \sum_k r_k\, \Pi[e_k], \qquad (4)$$

with $r_k := \langle e_k|\rho|e_k\rangle$ quantifying the projection of ρ onto the energy eigenstate $\lvert e_k\rangle$. The optimal, reversible, implementation of the ρ to η transfer was proposed in ref. [27] and it was shown that the "average" work extracted is $\langle W_{\text{ext}}\rangle = k_B T\,(S_{\text{vN}}(\eta) - S_{\text{vN}}(\rho)) \geq 0$, where S_{vN} is the Von Neumann entropy, defined as $S_{\text{vN}}(\rho) := -\text{tr}[\rho \log \rho]$. This is in agreement with equality in Eq. (2) assuming the free energy of a quantum nonequilibrium configuration is defined as $F(\rho, H) := \text{tr}[H\,\rho] - k_B T\, S_{\text{vN}}(\rho)$[46,47,53–55], and realizing that the state change ρ to η carries no energy change, $\Delta U = 0$, and hence $\Delta F = -k_B T\, \Delta S_{\text{vN}}$. We remark that only the "average" work was provided in ref. [27] but no distribution of work was given with respect to which $\langle W_{\text{ext}}\rangle$ is an "average".

Generalizing first the steps of the optimal protocol[27] to include irreversibility will allow us to investigate the impact of entropy production on distributions of work and heat below.

The new protocol consists of the following five steps, and the state evolution is visualized for a qubit in Fig. 1: (I) Use a unitary V to rotate the quantum system's configuration $(\rho, H^{(0)})$ into configuration $(\tilde{\rho}, H^{(0)})$ where $\tilde{\rho} := V\rho V^\dagger = \sum_l p_l \Pi[\tilde{\psi}_l]$. In the reversible protocol, V is chosen such that $\lvert\tilde{\psi}_l\rangle := V\lvert\psi_l\rangle$ is a Hamiltonian eigenstate, i.e., $[\tilde{\rho}, H^{(0)}] = 0$[27]. Here we allow V to be imperfect and hence $[\tilde{\rho}, H^{(0)}] \neq 0$; (II) Change the Hamiltonian rapidly resulting in a quench from $(\tilde{\rho}, H^{(0)})$ to $(\tilde{\rho}, H^{(1)})$. In the reversible protocol, the energetic levels of $H^{(1)}$ are chosen such that the configuration $(\tilde{\rho}, H^{(1)})$ is thermal at temperature T[27]. This is possible because we assume that we can perform arbitrary quenches of the Hamiltonian, and since the initial state ρ has full rank, there exists some Hamiltonian with respect to which an energy incoherent state $\tilde{\rho}$ will be thermal. Here we consider the case that the energetic levels of $H^{(1)}$ are adjusted imperfectly, and hence configuration $(\tilde{\rho}, H^{(1)})$ is not necessarily thermal even if $[\tilde{\rho}, H^{(1)}] = 0$; (III) Put the quantum system in thermal contact with a heat bath at temperature T, and wait for a sufficiently long time so that $(\tilde{\rho}, H^{(1)})$ is brought into the thermal configuration $(\tau_1, H^{(1)})_T$; (IV) Change the system's Hamiltonian slowly from $H^{(1)}$ to $H^{(N)}$, keeping the system in thermal contact with the heat bath. The evolution is chosen quasi-static (i.e., very slow), such that thermal equilibrium at T is maintained throughout this step. The final Hamiltonian $H^{(N)}$ is chosen so that the system's thermal state is the desired final state, i.e., $\tau_N = \eta$; (V) Decouple the system from the thermal bath and quench the Hamiltonian back to $H^{(0)}$, changing the system's configuration from $(\eta, H^{(N)})_T$ to the desired configuration $(\eta, H^{(0)})$.

Since Steps (I), (II), (IV), and (V) are either unitary or quasi-static, they are thermodynamically reversible. The thermodynamic irreversibility of the protocol occurs when the quantum system is put in contact with the thermal bath in Step (III). The irreversible thermalization $(\tilde{\rho}, H^{(1)}) \to (\tau_1, H^{(1)})_T$ leads to a reduction in free energy, i.e., $\Delta F^{(\text{III})} = -k_B T\, D[\tilde{\rho}\|\tau_1]$ where $D[\tilde{\rho}\|\tau_1] = \text{tr}[\tilde{\rho}(\log\tilde{\rho} - \log\tau_1)] \geq 0$ is the quantum relative entropy between the state before thermalization, $\tilde{\rho}$, and the state after thermalization, τ_1, which vanishes if and only if $\tilde{\rho} = \tau_1$. Observing that no work is exchanged during thermalization ($W_{\text{ext}} = 0$), and based on the assumption that Eq. (2) holds in the
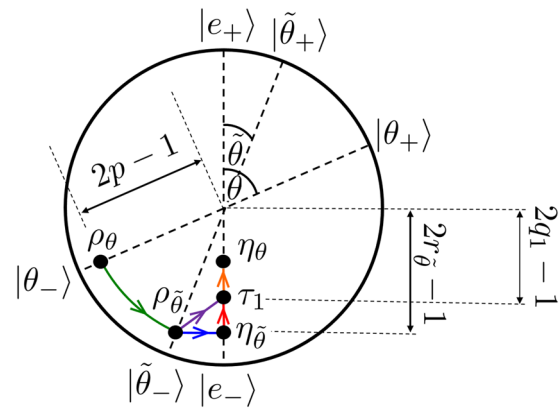

Fig. 1 State evolution during work extraction protocol for qubits. Initially, the system is prepared in state ρ_θ and is then unitarily evolved to $\rho_{\tilde{\theta}}$ (green arrow) which has the eigenstates $\lvert\tilde{\theta}_\pm\rangle$. Following a Hamiltonian quench that changes the splitting of the energetic levels but does not alter the energy eigenstates $\lvert e_\pm\rangle$, the system is put in thermal contact with a bath and allowed to relax to the thermal state τ_1. The full thermalization step (purple arrow) can be split into quantum decoherence with respect to the energy eigenbasis (blue arrow) $\rho_{\tilde{\theta}} \mapsto \eta_{\tilde{\theta}}$ followed by classical thermalization (red arrow) $\eta_{\tilde{\theta}} \mapsto \tau_1$. Next, the state transfer $\tau_1 \mapsto \eta_\theta$ (orange arrow) is effected by a quasi-static isothermal process. Finally, the Hamiltonian is quenched back to its initial configuration. This protocol realizes the thermodynamic removal of coherences, i.e., transforming ρ_θ to η_θ, while irreversibility arises due to the mismatches between $\rho_{\tilde{\theta}}$ and $\eta_{\tilde{\theta}}$ as well as $\eta_{\tilde{\theta}}$ and τ_1.

quantum regime, the term $k_B D[\tilde{\rho}\|\tau_1]$ is often identified with the entropy $S_{\text{irr}}^{(\text{III})}$ that is produced during the thermalization step[35,56].

As recently discussed in ref. [34,35], the geometric measure of irreversibility given by the relative entropy splits into a quantum and a classical part,

$$D[\tilde{\rho}\|\tau_1] = D[\tilde{\rho}\|\tilde{\eta}] + D[\tilde{\eta}\|\tau_1], \qquad (5)$$

where in analogy with Eq. (4), we define $\tilde{\eta} := \sum_k \Pi[e_k]\,\tilde{\rho}\,\Pi[e_k]$. As we will show below, Eq. (5) can be obtained as averages over the entropy produced along decoherence trajectories and classical thermalization trajectories[35]. This splitting reflects the fact that the quantum configuration $(\tilde{\rho}, H^{(1)})$ is out of equilibrium in two distinct ways: it can have quantum coherences between energy levels, and classical non-thermality due to non-Boltzmann probabilities for the energies. In particular, $D[\tilde{\rho}\|\tilde{\eta}] \equiv S_{\text{vN}}(\tilde{\eta}) - S_{\text{vN}}(\tilde{\rho})$ is known in the literature as the "relative entropy of coherence" which quantifies the coherence (or asymmetry) of the state $\tilde{\rho}$ with respect to the Hamiltonian $H^{(1)}$[57,58]. Similarly, $D[\tilde{\eta}\|\tau_1]$ can be seen as a measure of classical non-thermality.

A special case: qubits. For the special case of qubits, we may provide an intuitive illustration of the protocol in a geometric fashion by use of the Bloch sphere. Specifically, we shall denote the jth Hamiltonians as $H^{(j)} := \frac{1}{2}\hbar\omega_j(\Pi[e_+] - \Pi[e_-])$, and represent the initial and unitarily evolved states, ρ and $\tilde{\rho}$, in terms of angles θ and $\tilde{\theta}$, respectively:

$$\rho \equiv \rho_\theta := p\Pi[\theta_-] + (1-p)\Pi[\theta_+], \qquad \tilde{\rho} \equiv \rho_{\tilde{\theta}} := p\Pi[\tilde{\theta}_-] + (1-p)\Pi[\tilde{\theta}_+],$$

$$(6)$$

where $1 > p > \frac{1}{2}$, and

$$\lvert\theta_\pm\rangle := \cos(\theta/2)\lvert e_\pm\rangle \pm e^{\pm i\phi}\sin(\theta/2)\lvert e_\mp\rangle,$$
$$\lvert\tilde{\theta}_\pm\rangle := \cos(\tilde{\theta}/2)\lvert e_\pm\rangle \pm e^{\pm i\phi}\sin(\tilde{\theta}/2)\lvert e_\mp\rangle. \qquad (7)$$

We note that, without loss of generality, we may assume that $\phi = \tilde{\phi} = 0$ due to the invariance of the work extraction protocol with respect to unitary evolution generated by H, while θ and $\tilde{\theta}$ may be assumed to fall in the range $[-\pi/2, \pi/2]$, since angles outside this range would be accounted for by changing the sign of the Hamiltonian. The decohered state η is thus defined as $\eta_\theta = r_\theta \Pi[e_-] + (1 - r_\theta) \Pi[e_+]$ with $r_\theta := \langle e_- | \rho_\theta | e_- \rangle$, and $\eta_{\tilde{\theta}}$ is similarly defined. The imperfect work extraction protocol for qubits is depicted in Fig. 1.

As stated above, the geometric distance between $\rho_{\tilde{\theta}}$ and the equilibrium state can be split into a coherence term and classical non-thermality term as per Eq. (5). These are shown by the blue and red arrows in Fig. 1, respectively. Below, we shall offer an intuitive quantification of coherence and classical non-thermality of the state $\rho_{\tilde{\theta}}$, named *coh* and *nonth* respectively, so that $coh(\rho_{\tilde{\theta}}) = nonth(\rho_{\tilde{\theta}}) = 0$ if and only if $\rho_{\tilde{\theta}} = \tau_1$. These will be useful parameters in terms of which we may present our results later in the paper.

The coherence of $\rho_{\tilde{\theta}}$ with respect to the Hamiltonian can be quantified by the minimum overlap between the eigenstates of $\rho_{\tilde{\theta}}$ and the eigenstates of $H^{(1)}$, i.e.,

$$coh(\rho_{\tilde{\theta}}) := \min_{k,l} |\langle e_k | \tilde{\theta}_l \rangle|^2 = |\langle e_+ | \tilde{\theta}_- \rangle|^2 = \sin^2(\tilde{\theta}/2). \quad (8)$$

Hence $coh(\rho_{\tilde{\theta}}) = 0$ for $\tilde{\theta} = 0$, and it monotonically increases as $|\tilde{\theta}| \to \pi/2$, saturating at its maximum value of $coh(\rho_{\pi/2}) = 1/2$. The classical non-thermality of the qubit state $\rho_{\tilde{\theta}}$ compared with the thermal state τ_1 for $H^{(1)}$ can be quantified by the logarithm of the ratio of ground state probabilities, i.e.,

$$nonth(\rho_{\tilde{\theta}}) := \log \frac{q_1}{r_{\tilde{\theta}}}, \quad (9)$$

where $q_1 := \langle e_- | \tau_1 | e_- \rangle$ and $r_{\tilde{\theta}} = \langle e_- | \rho_{\tilde{\theta}} | e_- \rangle = \langle e_- | \eta_{\tilde{\theta}} | e_- \rangle$ are the ground state populations of τ_1 and $\rho_{\tilde{\theta}}$, respectively, see Fig. 1. Hence $nonth(\rho_{\tilde{\theta}}) = 0$ when $q_1 = r_{\tilde{\theta}}$, while a positive (negative) $nonth(\rho_{\tilde{\theta}})$ corresponds to a lower (higher) ground state population in $\rho_{\tilde{\theta}}$ than that of the thermal state τ_1, corresponding to a down (up) red arrow in Fig. 1.

Stochastic quantum trajectories. Working on the level of density matrices of the system during the protocol (see Fig. 1 for the qubit example) limits the discussion of thermodynamic quantities to macroscopic expectation values only. In contrast, stochastic thermodynamics associates heat $Q(\Gamma)$, work $W(\Gamma)$, and entropy production $s_{\mathrm{irr}}(\Gamma)$ to individual microscopic trajectories Γ forming the set of possible system evolutions[59,60]. In this more detailed picture the macroscopic thermodynamic quantities $\langle Q \rangle$, $\langle W \rangle$, and $\langle S \rangle$ arise as weighted averages over these trajectories. In the quantum regime, quantum stochastic thermodynamics captures the set of possible trajectories that, in addition to classical trajectories, are determined by quantum coherences and nonthermal sources of stochasticity[36,38,61–64]. These trajectories consist of time-sequences of pure quantum states taken by an open system in a single run of an experiment.

One way to experimentally "see" quantum trajectories is by observing a sequence of stochastic outcomes of a generalized measurement performed on a system[65]. Immense experimental progress in the ability to measure quantum states with high efficiency has enabled the observation of individual jumps in photon number, and more recently the tracking of single quantum trajectories of superconducting qubits[33,66–68]. The natural set of quantum trajectories is a function of how the system is measured, and various quantum trajectory sets have been discussed in the literature each corresponding to different measurement setups: the so-called "unravelings"[69,70]. Averaging

the system's pure states over many experimental runs then gives back the density matrix describing the system's mixed state, whose evolution is governed by completely positive, trace preserving maps, also known as a quantum channel. Using the methods of quantum stochastic thermodynamics we here access a system's fluctuations in work, heat, and entropy production, when quantum coherences are involved and irreversibility occurs. This allows us to expose the microscopic links between irreversibility and energetic exchanges in the quantum regime.

We here use "eigenstate trajectories" that describe a system that travels through a sequence of eigenstates of its time-local density operators. Namely, the system is measured at instances in time $j = 1, 2, \ldots$ in the instantaneous eigenbases of the states ρ_j that are assumed to be known, for example, from a master equation that describes the open system dynamics. We note that this is an idealized scenario as in general one does not know what the density operators ρ_j are and cannot guarantee to measure in the correct eigenbases. The eigenstate trajectories are analytically tractable, and provide a convenient analytical tool to investigate the energetic footprints of irreversibility, as we will see below.

The ensemble of trajectories $\{\Gamma\}$ taken by a quantum system when undergoing the work extraction protocol outlined in the previous section can be broken up into trajectories for each of the Steps (see Fig. 2 for the qubit example). We will here focus on discussing the thermalization of the system in Step (III), for which the initial density matrix $\tilde{\rho}$ can host coherences $D[\tilde{\rho}||\tilde{\eta}] > 0$ and classical non-thermality $D[\tilde{\eta}||\tau_1] > 0$ at the point when it is brought in contact with the thermal bath. The trajectories for the full protocol are detailed in the "Methods".

The thermalization process in Step (III) may be described by the quantum channel $\Lambda(\rho) := \mathrm{tr}_\mathcal{B}[\mathcal{V}(\rho \otimes \tau_\mathcal{B})\mathcal{V}^\dagger]$, where $\tau_\mathcal{B} := \exp(-H_\mathcal{B}/k_B T)/Z_\mathcal{B}$ is the initial thermal state of the bath with Hamiltonian $H_\mathcal{B}$ and partition function $Z_\mathcal{B}$, and $\mathcal{V}$ is a unitary operator that commutes with $H^{(1)} + H_\mathcal{B}$. Hence Λ is a thermal operation[71–73]. We further demand that Λ is a fully thermalizing map, i.e., $\Lambda(\rho) = \tau_1$ for all ρ. This map exists, for example, when the bath is chosen as an infinite ensemble of identical particles, each with the same Hamiltonian as the system, and with $\mathcal{V}$ implementing a sequence of partial swaps between the system and each bath particle, or a full swap with just a single particle[74]. Minimal trajectories for the thermalization process can now be constructed as $\Gamma^{(\mathrm{III})}_{(l,n)} \equiv |\tilde{\psi}_l\rangle \mapsto |e_n\rangle$ (see Fig. 2 for the specific case where the system is a qubit, with $|\tilde{\psi}_l\rangle \equiv |\tilde{\theta}_\pm\rangle$). The probability of this transfer to occur is $P(\Gamma^{(\mathrm{III})}_{(l,n)}) = \langle \tilde{\psi}_l | \tilde{\rho} | \tilde{\psi}_l \rangle \langle e_n | \Lambda(\Pi[\tilde{\psi}_l]) | e_n \rangle$, which is obtained by first projectively measuring the system with respect to the eigenbasis $|\tilde{\psi}_l\rangle$ of $\tilde{\rho}$, then applying the thermalization channel Λ, and finally measuring the system with respect to the eigenbasis $|e_n\rangle$ of τ_1. Since $\mathcal{V}$ commutes with the total Hamiltonian while $\tau_\mathcal{B}$ commutes with the bath Hamiltonian, it can be shown (see Theorem 1 in ref. [75]) that $\langle e_n | \Lambda(\Pi[\tilde{\psi}_l]) | e_n \rangle = \sum_m |\langle e_m | \tilde{\psi}_l \rangle|^2 \langle e_n | \Lambda(\Pi[e_m]) | e_n \rangle$, where $|e_m\rangle$ are eigenstates of the system Hamiltonian $H^{(1)}$. We may therefore "augment" our trajectories by projecting the system onto the energy basis $|e_m\rangle$ first before letting it thermalize classically[64].

The augmented trajectories are denoted $\Gamma^{(\mathrm{III})}_{(l,m,n)} \equiv |\tilde{\psi}_l\rangle \mapsto |e_m\rangle \mapsto |e_n\rangle$, with probabilities

$$P\left(\Gamma^{(\mathrm{III})}_{(l,m,n)}\right) = \langle \tilde{\psi}_l | \tilde{\rho} | \tilde{\psi}_l \rangle |\langle e_m | \tilde{\psi}_l \rangle|^2 \langle e_n | \tau_1 | e_n \rangle. \quad (10)$$

It can be shown that the minimal trajectories $\Gamma^{(\mathrm{III})}_{(l,n)}$ and the augmented trajectories $\Gamma^{(\mathrm{III})}_{(l,m,n)}$ are thermodynamically equivalent, as they result in the same entropy production (see "Methods" for details). However, the augmented trajectories have the benefit of
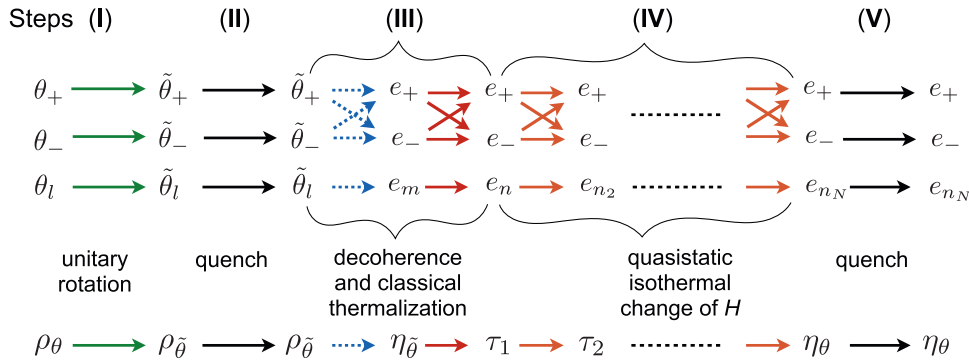
Fig. 2 Pure-state qubit trajectories for the work extraction protocol. Illustration of the evolution of the qubit during the work protocol on the trajectory level and on the density matrix level. The qubit's trajectories are deterministic during Steps (I) (unitary, green arrows), (II) (quench, black arrows), and (V) (quench, black arrows), i.e., they take one state to a unique other state. In contrast, during the decoherence part in Step (III) (blue dashed arrows) the qubit stochastically jumps from one of the states $|\tilde{\theta}_\pm\rangle$ to one of the energy eigenstates $|e_\pm\rangle$, thus losing any quantum coherence in an irreversible manner. During the classical thermalization part in Step (III) (red arrows) the qubit stochastically jumps from one of the energy eigenstates to another energy eigenstate, thus losing any classical non-thermality in an irreversible manner. The qubit's trajectories during the classical quasi-static isothermal change of H (Step (IV), orange arrows), are stochastic but reversible, due to infinitely small thermalizations taking place throughout.

naturally splitting into a "decoherence trajectory" $\Gamma^{\mathrm{q}}_{(l,m)} \equiv |\tilde{\psi}_l\rangle \mapsto |e_m\rangle$, followed by a "classical thermalization trajectory" $\Gamma^{\mathrm{cl}}_{(m,n)} \equiv |e_m\rangle \mapsto |e_n\rangle$, as depicted in Fig. 2 for the qubit case. Their probabilities to occur are

$$P\left(\Gamma^{\mathrm{q}}_{(l,m)}\right) = \sum_n P\left(\Gamma^{(\mathrm{III})}_{(l,m,n)}\right) = \langle\tilde{\psi}_l|\tilde{\rho}|\tilde{\psi}_l\rangle|\langle e_m|\tilde{\psi}_l\rangle|^2, \quad (11)$$

and

$$P\left(\Gamma^{\mathrm{cl}}_{(m,n)}\right) = \sum_l P\left(\Gamma^{(\mathrm{III})}_{(l,m,n)}\right) = \langle e_m|\tilde{\eta}|e_m\rangle\langle e_n|\tau_1|e_n\rangle, \quad (12)$$

respectively which can be obtained as marginals of the probability distribution given by Eq. (10) (see "Methods" for details). Here $\Gamma^{\mathrm{q}}_{(l,m)}$ are the trajectories the system undertakes as it undergoes the decoherence process $\tilde{\rho} \mapsto \tilde{\eta}$, while $\Gamma^{\mathrm{cl}}_{(m,n)}$ are the trajectories that the system undertakes as it undergoes the classical thermalization process $\tilde{\eta} \mapsto \tau_1$.

We note that while ref. [35] also considered augmented trajectories to separate the quantum and classical contributions to the stochastic entropy production, these constituted of the initial and final energy eigenstates of the bath, together with initial and final eigenstates of the system, neither of which are assumed to be energy eigenstates. In our approach, the assumption that $\Lambda(\tilde{\rho})$ is energy incoherent allows for the heat exchange of the process, in addition to the entropy production, to be split into a quantum and classical component, which we discuss below.

Stochastic quantum entropy production. Within quantum stochastic thermodynamics the entropy production along a quantum trajectory Γ is

$$s_{\mathrm{irr}}(\Gamma) := k_B \log \frac{P(\Gamma)}{P^*(\Gamma^*)}, \quad (13)$$

exposing the entropy production's microscopic origin as the imbalance between the probabilities $P(\Gamma)$ and $P^*(\Gamma^*)$ of a forward trajectory Γ and its corresponding backward trajectory Γ^*, respectively[38,64]. The backward trajectory Γ^* can be understood as the time-reversed sequence of eigenstates which constitute the forward trajectory Γ. In order to evaluate the probability for the backward trajectory of the thermalization Step (III), we consider the time-reversed process as one where the system and environment are initially in the compound state $\tau_1 \otimes \tau_B$, i.e., the system starts in the average state that it took at the end of the

forward process, while the bath is in thermal equilibrium. On this initial product state, the time-reverse of the forward evolution of system and bath is applied, and projections are performed in reversed order into the forward eigenstates $|\tilde{\psi}_l\rangle$ and $|e_m\rangle$. This leads to Kraus operators given in (47) which describe the time-reversed trajectories, see "Methods".

We find that the stochastic entropy production for the thermalization Step (III) can be expressed as

$$s_{\mathrm{irr}}\left(\Gamma^{(\mathrm{III})}\right) = s^{\mathrm{qu}}_{\mathrm{irr}}\left(\Gamma^{\mathrm{q}}_{(l,m)}\right) + s^{\mathrm{cl}}_{\mathrm{irr}}\left(\Gamma^{\mathrm{cl}}_{(m,n)}\right), \quad (14)$$

where we identify

$$s^{\mathrm{qu}}_{\mathrm{irr}}\left(\Gamma^{\mathrm{q}}_{(l,m)}\right) = k_B \log \frac{\langle\tilde{\psi}_l|\tilde{\rho}|\tilde{\psi}_l\rangle}{\langle e_m|\tilde{\eta}|e_m\rangle} \quad (15)$$

as the stochastic quantum entropy production, and

$$s^{\mathrm{cl}}_{\mathrm{irr}}\left(\Gamma^{\mathrm{cl}}_{(m,n)}\right) = k_B \log \frac{\langle e_m|\tilde{\eta}|e_m\rangle}{\langle e_m|\tau_1|e_m\rangle} \quad (16)$$

as the stochastic classical entropy production. Since the probability of the augmented trajectories, $P(\Gamma^{(\mathrm{III})}_{(l,m,n)})$, gives $P(\Gamma^{\mathrm{q}}_{(l,m)})$ and $P(\Gamma^{\mathrm{cl}}_{(m,n)})$ as marginals (see Eqs. (11) and (12)), the average entropy production in Step (III) can also be split into an average quantum entropy production $\langle s^{\mathrm{qu}}_{\mathrm{irr}}\rangle$, and an average classical entropy production, $\langle s^{\mathrm{cl}}_{\mathrm{irr}}\rangle$. One finds, see "Methods", that each of these averages reduces to a relative entropy between two pairs of system states,

$$\langle s^{\mathrm{qu}}_{\mathrm{irr}}\rangle = \sum_{l,m} P\left(\Gamma^{\mathrm{q}}_{(l,m)}\right) s^{\mathrm{qu}}_{\mathrm{irr}}\left(\Gamma^{\mathrm{q}}_{(l,m)}\right) = k_B D[\tilde{\rho}||\tilde{\eta}], \quad (17)$$

$$\langle s^{\mathrm{cl}}_{\mathrm{irr}}\rangle = \sum_{m,n} P\left(\Gamma^{\mathrm{cl}}_{(m,n)}\right) s^{\mathrm{cl}}_{\mathrm{irr}}\left(\Gamma^{\mathrm{cl}}_{(m,n)}\right) = k_B D[\tilde{\eta}||\tau_1]. \quad (18)$$

This shows that the relative entropies $D[\tilde{\rho}||\tilde{\eta}]$ and $D[\tilde{\eta}||\tau_1]$, which geometrically link density matrices, are physically meaningful as the average entropy productions associated with the evolution of the quantum system along ensembles of quantum trajectories. The two separate contributions to the entropy production arise because the system has two distinct nonequilibrium features, coherence with reference to the Hamiltonian, and classical non-thermality. Each is irreversibly removed when the system is brought into contact with the thermal bath and undergoes decoherence trajectories followed by classical thermalization trajectories.

Finally, we show in "Methods" that the average entropy production for the full protocol reduces to $\langle s_{irr}^{qu}\rangle + \langle s_{irr}^{cl}\rangle$ in the limit where Step (IV) becomes a quasi-static process, i.e., in this limit the average entropy production for the full protocol coincides with the average entropy production for the thermalization step alone.

Classical and quantum heat distributions. We now analyze the energetic fluctuations of the quantum decoherence and classical thermalization trajectories, $\Gamma_{(l,m)}^{q}$ and $\Gamma_{(m,n)}^{cl}$, respectively. Since no external control is applied during these trajectories, such as a change of Hamiltonian, no work is done on the system and hence the energetic changes of the system consist entirely of heat. But since we identified two contributions to irreversibility, namely quantum decoherence and classical thermalization, it stands to reason that we should obtain two types of heat[36,37].

The microscopic mechanisms associated with classical thermalization of the system with the bath are the quantum jumps from $|e_m\rangle$ to $|e_n\rangle$, which give rise to energetic fluctuations. The heat the system absorbs from the bath is

$$Q_{cl}\left(\Gamma_{(m,n)}^{cl}\right) = E_n^{(1)} - E_m^{(1)}, \qquad (19)$$

where $E_k^{(j)} := \langle e_k|H^{(j)}|e_k\rangle$, which is the standard classical stochastic heat. We note that Step (IV) also incurs classical heat, but we do not discuss this contribution here, as the stochastic thermodynamic description is well established for heat exchanges during this classical quasi-static isothermal process[59,60].

On the other hand, the microscopic mechanisms associated with decoherence are the quantum jumps from $|\tilde{\psi}_l\rangle$ to $|e_m\rangle$, which give rise to energetic fluctuations of the system that are entirely quantum mechanical. The system's energy increase due to decoherence is

$$Q_{qu}\left(\Gamma_{(l,m)}^{q}\right) = E_m^{(1)} - \langle\tilde{\psi}_l|H^{(1)}|\tilde{\psi}_l\rangle. \qquad (20)$$

It has no classical counterpart and is hence referred to as quantum heat[36,37]. Contrary to the classical stochastic heat which has fixed quantized values given by the Hamiltonian $H^{(1)}$ alone, the stochastic quantum heat's values vary as a function of the eigenbasis of the state $\tilde{\rho}$. When this state has no quantum coherences ($D[\tilde{\rho}||\tilde{\eta}] = 0$) the only realized value of the stochastic quantum heat is 0, i.e., in the absence of coherences, decoherence has no effect on the system's state and no energetic fluctuations result from it. Fluctuations of the quantum heat take place as soon as $D[\tilde{\rho}||\tilde{\eta}] > 0$. Histograms of the classical stochastic heat Q_{cl} and the quantum heat Q_{qu} for the qubit model are shown in Fig. 3a, b for states $\rho_{\tilde{\theta}}$ that have only classical non-thermality while $coh = 0$, and states that have only coherences while $nonth = 0$, respectively.

Note that we were able to split the energetic changes of the thermalization process into Eqs. (19) and (20) by first augmenting the minimal trajectories $\Gamma_{(l,n)}^{(III)}$ to $\Gamma_{(l,m,n)}^{(III)}$, and then splitting these into a decoherence trajectory $\Gamma_{(l,m)}^{q}$ followed by a classical thermalization trajectory $\Gamma_{(m,n)}^{cl}$. While the minimal trajectories only consider transitions between the system's time-local eigenbases, and the projective measurements which realize them are therefore "non-invasive", the same is not true for the augmented trajectories which require a projective energy measurement on the system prior to thermalization, which destroys any coherence present. Notwithstanding, since this energy measurement does not alter the stochastic entropy production one can consider it as a "virtual process" that need
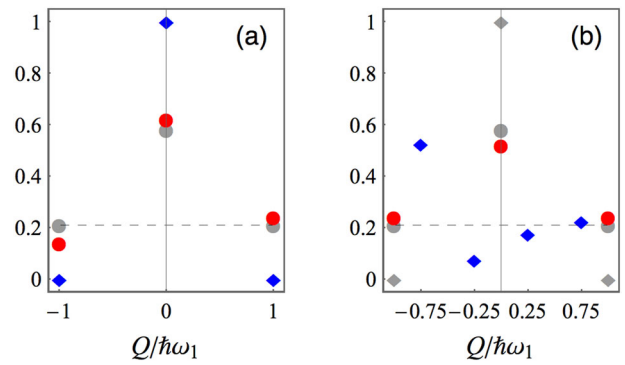

Fig. 3 Heat distributions for a qubit undergoing the thermalization Step (III). Histograms of classical heat Q_{cl} (red circles) and quantum heat Q_{qu} (blue squares) for **a** an initial state $\rho_{\tilde{\theta}}$ that hosts classical non-thermality: $nonth(\rho_{\tilde{\theta}}) = \log(0.2/0.3)$ and $coh(\rho_{\tilde{\theta}}) = 0$, and for **b** an initial state $\rho_{\tilde{\theta}}$ that hosts quantum coherence: $coh(\rho_{\tilde{\theta}}) = \sin^2(\pi/6) = 1/4$ and $nonth(\rho_{\tilde{\theta}}) = 0$. For comparison, gray circles and gray diamonds in both panels show the classical and quantum heat histograms, respectively, for when Step (III) is fully reversible, i.e., $\rho_{\tilde{\theta}} = \tau_1$ and hence $coh(\rho_{\tilde{\theta}}) = 0 = nonth(\rho_{\tilde{\theta}})$. Note that even then the system can exchange heat with the bath leading to a classical heat distribution with non-zero but symmetrical values (dashed line) that give a zero average classical heat. In **a** the only quantum heat value with non-zero probability is 0 (no quantum heat when thermalizing a classical state), while in **b** four nontrivial quantum heat values occur since $coh(\rho_{\tilde{\theta}}) \neq 0$.

not be actually performed. But to physically observe the quantum heat distribution would necessitate such an energy measurement, and then the source of the quantum heat originates from the projective energy measurement itself, and not from the thermal bath, as first discussed in ref. [36].

Heat footprints of classical and quantum irreversibility. We are now ready to discuss the energetic footprints of irreversibility in the quantum regime. The energetic footprints of classical entropy production during Step (III) are made immediately apparent from the stochastic equation (16) which, in conjunction with the classical heat value given by Eq. (19), can be re-expressed as

$$s_{irr}^{cl}\left(\Gamma_{(m,n)}^{cl}\right) = k_B\log\frac{\langle e_m|\tilde{\eta}|e_m\rangle}{\langle e_n|\tau_1|e_n\rangle} - \frac{Q_{cl}\left(\Gamma_{(m,n)}^{cl}\right)}{T}. \qquad (21)$$

When averaged over the classical thermalization trajectories $\Gamma_{(m,n)}^{cl}$, the above expression links the average absorbed heat $\langle Q_{cl}\rangle$ to the average entropy production $\langle s_{irr}^{cl}\rangle$ as

$$\langle s_{irr}^{cl}\rangle = k_B(S_{vN}(\tau_1) - S_{vN}(\tilde{\eta})) - \frac{\langle Q_{cl}\rangle}{T}. \qquad (22)$$

This thermodynamic equality, going back to Clausius, is the well-known energetic footprint of entropy production in the classical regime. It can be used to define the irreversibly dissipated heat,

$$\langle Q_{diss}^{sur}\rangle := -\langle Q_{cl}\rangle + T\Delta S_{cl} = T\langle s_{irr}^{cl}\rangle = k_B T \, D[\tilde{\eta}||\tau_1] \geq 0, \qquad (23)$$

which is strictly positive when the entropy production $\langle s_{irr}^{cl}\rangle$ is non-zero, which arises when forward and backwards probabilities of the process deviate, see Eq. (13). In other words, the energetic footprint of non-zero $\langle Q_{diss}^{sur}\rangle$ gives thermodynamic testament of the arrow of time.

Meanwhile, the stochastic quantum entropy production $s_{irr}^{qu}(\Gamma_{(l,m)}^{q})$ in Eq. (15) is given purely by a stochastic quantum entropy change and does not appear to involve any contributions

from the stochastic quantum heat Q_{qu} whatsoever. When averaged over all quantum decoherence trajectories, the quantum heat in fact vanishes, see "Methods",

$$\langle Q_{qu} \rangle_{\Gamma^q} = 0, \qquad (24)$$

while the average quantum entropy production can formally be rewritten as

$$\langle s_{irr}^{qu} \rangle = k_B(S_{vN}(\tilde{\eta}) - S_{vN}(\tilde{\rho})) - \frac{1}{T}\langle Q_{qu} \rangle.^{\;0} \qquad (25)$$

This quantum thermodynamic equality shows that the energetic footprint of quantum entropy production, i.e., a fixed relationship between average heat absorption and average entropy production, is mute in the quantum regime. This indicates a fundamental difference in how quantum and classical heat relate to the entropy production.

While prima faciae Eq. (25) seems to suggest that the quantum entropy production is completely dissociated from quantum heat, such a conclusion is premature. Indeed, on closer examination we discover that the average quantum entropy production $\langle s_{irr}^{qu} \rangle$ is intimately linked with the variance in quantum heat, $Var(Q_{qu})$, a quantity that has recently been connected to witnessing entanglement generation[51]. Specifically, we shall show that $\langle s_{irr}^{qu} \rangle = 0$ is both necessary and sufficient for $Var(Q_{qu}) = 0$, and for the special case of qubits, they are co-monotonic with energy coherence of the system's state. Before discussing this, let us first highlight that no such relationship exists between the average classical entropy production $\langle s_{irr}^{cl} \rangle$ and the variance in classical heat, $Var(Q_{cl})$; as shown in "Methods", the variance in classical heat as the system thermalizes to τ_1 takes the simple form of

$$Var(Q_{cl}) = \Delta(H^{(1)}, \tilde{\eta}) + \Delta(H^{(1)}, \tau_1) \equiv \Delta(H^{(1)}, \tilde{\rho}) + \Delta(H^{(1)}, \tau_1), \qquad (26)$$

where $\Delta(H, \rho) := tr[H^2 \rho] - tr[H\rho]^2$ is the variance of H in state ρ. Clearly, $\langle s_{irr}^{cl} \rangle = 0$ is neither necessary nor sufficient for $Var(Q_{cl}) = 0$: (i) $\langle s_{irr}^{cl} \rangle = 0$ if and only if $\tilde{\eta} = \tau_1$, whereas in such a case $Var(Q_{cl}) = 2\Delta(H^{(1)}, \tau_1) \geq 0$ with equality being achieved only in the limit of zero temperature; (ii) $Var(Q_{cl}) = 0$ if and only if $\Delta(H^{(1)}, \tilde{\eta}) = \Delta(H^{(1)}, \tau_1) = 0$. This means that both $\tilde{\eta}$ and τ_1 only have support on a single energy subspace of the Hamiltonian, such energy subspace of τ_1 necessarily being the lowest one. However, if the subspace of $\tilde{\eta}$ is disjoint from that of τ_1, then $\langle s_{irr}^{cl} \rangle = k_B D[\tilde{\eta}||\tau_1] = \infty$.

As shown in "Methods", the variance in quantum heat for the state $\tilde{\rho} = \sum_l p_l \Pi[\tilde{\psi}_l]$ decohering with respect to the Hamiltonian $H^{(1)}$ is the average variance of $H^{(1)}$ in the pure states $|\tilde{\psi}_l\rangle$, i.e.,

$$Var(Q_{qu}) = \sum_l p_l \Delta(H^{(1)}, \tilde{\psi}_l) \equiv \sum_l p_l I_\alpha(H^{(1)}, \tilde{\psi}_l), \qquad (27)$$

where $I_\alpha(H, \rho) := tr[H^2 \rho] - tr[H \rho^\alpha H \rho^{1-\alpha}]$ for $\alpha \in (0, 1)$ is the set of Wigner–Yanase–Dyson skew informations of the observable H in the state ρ[76–78]. This variance in quantum heat obeys the inequalities

$$\Delta(H^{(1)}, \tilde{\rho}) \geq Var\left(Q_{qu}\right) \geq I_\alpha(H^{(1)}, \tilde{\rho}), \qquad (28)$$

where the equalities in Eq. (28) are saturated when $\tilde{\rho}$ is a pure state.

Both $I_\alpha(H^{(1)}, \tilde{\rho})$ and $\langle s_{irr}^{qu} \rangle / k_B = D[\tilde{\rho}||\tilde{\eta}]$ quantify the asymmetry of the state $\tilde{\rho}$ with reference to the Hamiltonian $H^{(1)}$, and are thus linked with the resource theory of asymmetry[57,58,79–82]. Specifically, both $I_\alpha(H^{(1)}, \tilde{\rho})$ and $D[\tilde{\rho}||\tilde{\eta}]$ vanish if and only if $\tilde{\rho}$ commutes with $H^{(1)}$, and monotonically decrease under Hamiltonian-covariant quantum channels, i.e., quantum channels

$\mathcal{E}$ which satisfy $\mathcal{E}(e^{-itH^{(1)}}\rho e^{itH^{(1)}}) = e^{-itH^{(1)}}\mathcal{E}(\rho)e^{itH^{(1)}}$ for all $t \in \mathbb{R}$ and ρ. Therefore, by Eq. (27) we conclude that the average quantum entropy production vanishes if and only if the variance in quantum heat vanishes. In addition, given a pair of quantum states $\tilde{\rho}_1$ and $\tilde{\rho}_2 = \mathcal{E}(\tilde{\rho}_1)$, then: (a) the average quantum entropy production as $\tilde{\rho}_1$ decoheres to $\tilde{\eta}_1$ is no smaller than that obtained when $\tilde{\rho}_2$ decoheres to $\tilde{\eta}_2$; and (b) by Eq. (28), the lower bound to the quantum heat variance as $\tilde{\rho}_1$ decoheres to $\tilde{\eta}_1$ is no smaller than that obtained when $\tilde{\rho}_2$ decoheres to $\tilde{\eta}_2$. Of course, this observation still allows for the existence of a pair of states $\tilde{\rho}_1$ and $\tilde{\rho}_2 = \mathcal{E}(\tilde{\rho}_1)$ such that the average quantum entropy production of the former exceeds that of the latter, while the fluctuations in quantum heat of the latter exceeds that of the former. In what follows we shall show that, surprisingly, in the special case of qubits, i.e., $d = 2$, the fluctuations in quantum heat are monotonic with the average quantum entropy production. This link is twofold: (i) for two states with the same probability spectrum, but different eigenbases, the average quantum entropy production and the variance in quantum heat are monotonically increasing with the "energy coherence" of the eigenbasis; (ii) both the average quantum entropy production and the variance in quantum heat monotonically decrease under the action of Hamiltonian-covariant channels that are a combination of dephasing and depolarization. Both of these necessary links break down for higher dimensions, which we illustrate with a simple counter example for $d = 3$, see Fig. 4.

Let us first consider how $Var(Q_{qu})$ and $\langle s_{irr}^{qu} \rangle$ are affected by the relationship between the eigenbasis of the quantum state $\tilde{\rho}$, and the eigenbasis of the Hamiltonian $H^{(1)}$. Specifically, we shall consider a family of quantum states $\tilde{\rho}(\Theta) := \mathcal{U}(\Theta)\tilde{\rho}\,\mathcal{U}^\dagger(\Theta)$ for $\Theta \in [0, 1]$, where $\tilde{\rho} = \sum_l p_l \Pi[e_l]$ commutes with the Hamiltonian, with the one-parameter unitary operator

$$\mathcal{U} : [0, 1] \ni \Theta \mapsto \exp(\Theta \log \mathcal{F}), \qquad (29)$$

being generated by the discrete quantum Fourier transform[83] $\mathcal{F}$ defined as

$$\mathcal{F} : |e_l\rangle \mapsto |\xi_l\rangle := \frac{1}{\sqrt{d}}\sum_{k=1}^d e^{2\pi i(l-1)(k-1)}|e_k\rangle. \qquad (30)$$

It is simple to verify that $\{|e_k\rangle\}$ and $\{|\xi_l\rangle\}$ is a pair of mutually unbiased bases, with the energy coherence of $\{|\xi_l\rangle\}$ taking the maximum value of $coh := \min_{k,l}|\langle e_k|\xi_l\rangle|^2 = 1/d$. We shall denote the eigenbasis of $\tilde{\rho}(\Theta)$ as $\mathcal{B}(\Theta) := \{|\psi_l^\Theta\rangle \equiv \mathcal{U}(\Theta)|e_l\rangle\}$, and the probability spectrum of $\tilde{\rho}(\Theta)$ and $\tilde{\eta}(\Theta) := \sum_k \Pi[e_k]\tilde{\rho}(\Theta)\Pi[e_k]$ as $\mathbf{p} := (p_l)_l$ and $\mathbf{r}(\Theta)$, respectively. The Hamiltonian $H^{(1)}$ will map $\mathcal{B}(\Theta)$ to the symmetric doubly stochastic matrix $M(\Theta)$, which has the matrix elements $M_{k,l}^{(\Theta)} := |\langle e_k|\mathcal{U}(\Theta)|e_l\rangle|^2$. Both the quantum heat variance and average quantum entropy production can be computed by knowledge of these matrix elements: the quantum entropy production can be computed as $\langle s_{irr}^{qu} \rangle = k_B(S_{vN}(\tilde{\eta}(\Theta)) - S_{vN}(\tilde{\rho}(\Theta))) \equiv k_B(\mathscr{H}(\mathbf{r}(\Theta)) - \mathscr{H}(\mathbf{p}))$, where $\mathscr{H}$ denotes the Shannon entropy, and $\mathbf{r}(\Theta) = M(\Theta)\mathbf{p}$; the variance in quantum heat can be computed, as Eq. (27), by

$$\Delta(H^{(1)}, \psi_l^\Theta) = \sum_{k=1}^d M_{k,l}^{(\Theta)}\left(E_k^{(1)} - \sum_{k'=1}^d M_{k',l}^{(\Theta)} E_{k'}^{(1)}\right)^2. \qquad (31)$$

When $d = 2$, we have $M_{k \neq l}^{(\Theta)} = \frac{1}{2}\sin^2(\Theta\pi/2) \equiv coh$ and $M_{l,l}^{(\Theta)} = 1 - \frac{1}{2}\sin^2(\Theta\pi/2) \equiv 1 - coh$, where we recall that $coh := \sin^2(\tilde{\theta}/2)$ for $\tilde{\theta} \in [-\pi/2, \pi/2]$ (see Eq. (8)). Consequently, by Eqs. (27) and (31), the variance in quantum heat takes the simple
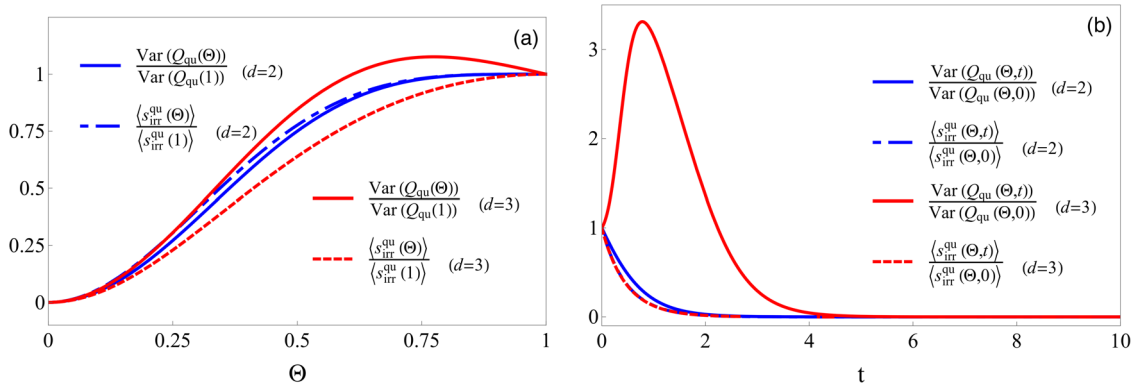
Fig. 4 Breakdown of monotonic relationship between quantum entropy production and fluctuations in quantum heat for dimensions greater than two. Here, we choose Hamiltonians with uniformly gapped spectra, i.e., $E_{k+1}^{(1)} - E_k^{(1)} = \hbar\omega_1$. The probability spectra for the states $\tilde{\rho}(\Theta)$ are chosen to be nondegenerate, but concentrated around $|\psi_1^\Theta\rangle$ and $|\psi_d^\Theta\rangle$. For $d = 2$, $p = (0.9, 0.1)$, while for $d = 3$, $p = (0.49, 0.04, 0.47)$. **a** Variance in quantum heat and average quantum entropy production as a function of Θ defined in Eq. (29). For $d = 2$, both $\mathrm{Var}(Q_{qu}(\Theta))$ and $\langle s_{irr}^{qu}(\Theta)\rangle$ monotonically increase as $\Theta \to 1$. For $d = 3$, however, while $\langle s_{irr}^{qu}(\Theta)\rangle$ monotonically increases with Θ, $\mathrm{Var}(Q_{qu}(\Theta))$ takes a maximum value at $\Theta \approx 0.8$, after which it decreases. **b** Here we choose the initial states $\tilde{\rho}(\Theta)$ with $\Theta = 0.3$, and evaluate $\mathrm{Var}(Q_{qu}(\Theta, t))$ and $\langle s_{irr}^{qu}(\Theta, t)\rangle$ for the states $e^{t\mathcal{L}}(\tilde{\rho}(\Theta))$ with $\mathcal{L}$ defined in Eq. (33). For $d = 2$, both $\mathrm{Var}(Q_{qu}(\Theta, t))$ and $\langle s_{irr}^{qu}(\Theta, t)\rangle$ monotonically decrease with t, while for $d = 3$, $\mathrm{Var}(Q_{qu}(\Theta, t))$ takes its maximum value at $t \approx 1$.

form of

$$\mathrm{Var}(Q_{qu}) = (\hbar\omega_1)^2 \left(coh - coh^2\right) \equiv \frac{(\hbar\omega_1)^2}{4}\sin^2(\tilde{\theta}), \qquad (32)$$

for all probability spectrums p (see "Methods" for details). As such, $\mathrm{Var}(Q_{qu})$ vanishes when $\Theta = 0 = coh$, and monotonically increases with Θ, or equivalently with coh, for all p and Hamiltonians $H^{(1)}$. As for the entropy production, we note that $D[\tilde{\rho}(0)||\tilde{\eta}(0)] = 0$, and that for any $\Theta_2 \geq \Theta_1$, there exists a Θ' such that $\boldsymbol{M}(\Theta_2) = \boldsymbol{M}(\Theta')\boldsymbol{M}(\Theta_1)$. Due to the properties of doubly stochastic matrices and majorization, this is a sufficient condition for $\mathscr{H}(\boldsymbol{r}(\Theta_2)) - \mathscr{H}(\boldsymbol{r}(\Theta_1)) \geq 0$, which implies that $\langle s_{irr}^{qu}\rangle$ also monotonically increases with Θ, or equivalently with coh, for all p and $H^{(1)}$[84–87]. The co-monotonic relationship between $\mathrm{Var}(Q_{qu})$ and $\langle s_{irr}^{qu}\rangle$ with Θ for qubits is demonstrated in Fig. 4a. Conversely, when $d = 3$ we see that while $\langle s_{irr}^{qu}\rangle$ monotonically increases with Θ, the same is not necessarily true for $\mathrm{Var}(Q_{qu})$ which in this instance takes a maximum value at $\Theta \approx 0.8$. Here, we have chosen the Hamiltonian to have a uniform spectral gap, i.e., $E_{k+1}^{(1)} - E_k^{(1)} = \hbar\omega_1$, with the nondegenerate probability spectrum p concentrated around $|\psi_1^\Theta\rangle$ and $|\psi_3^\Theta\rangle$. The reason for this is that $\Delta(H^{(1)}, \psi_l^\Theta)$ is maximized when the probability distribution $(M_{k,l}^{(\Theta)})_k$ is concentrated around the smallest and largest energy eigenvalues $E_1^{(1)}$ and $E_d^{(1)}$[88]. While this is certainly achieved at $\Theta = 1$ for qubits, this is no longer the case for larger systems, where $(M_{k,l}^{(1)})_k = (1/d, \dots, 1/d)$.

Next, we consider how $\mathrm{Var}(Q_{qu})$ and $\langle s_{irr}^{qu}\rangle$ are affected by a Hamiltonian-covariant quantum channel $\mathcal{E}$. As stated previously, $\langle s_{irr}^{qu}\rangle$ is known to monotonically decrease with applications of $\mathcal{E}$, i.e., for $\rho_2 = \mathcal{E}(\rho_1)$, $D[\rho_1||\eta_1] \geq D[\rho_2||\eta_2]$. Moreover, as shown in "Methods", so long as $\mathcal{E}$ is a convex combination of pure dephasing with respect to the Hamiltonian eigenbasis, and a depolarization channel which takes the system to the complete mixture, then for qubits $coh(\rho) \geq coh(\mathcal{E}(\rho))$ for all ρ. Consequently, by Eq. (32) the fluctuations in quantum heat for $\mathcal{E}(\rho)$ will be smaller than that of ρ. We demonstrate this in Fig. 4b for the Hamiltonian-covariant, Markovian dephasing channels

$$\mathcal{E}(\rho) = e^{t\mathcal{L}}(\rho), \text{ where}$$

$$\mathcal{L}(\rho) = \sum_k \Pi[e_k]\rho\Pi[e_k] - \frac{1}{2}\sum_k (\Pi[e_k]\rho + \rho\Pi[e_k]). \qquad (33)$$

It is simple to verify that $\langle e_k|e^{t\mathcal{L}}(\rho)|e_l\rangle = e^{-t(1-\delta_{l,k})}\langle e_k|\rho|e_l\rangle$, and so $e^{-iHt'}e^{t\mathcal{L}}(\rho)e^{iHt'} = e^{t\mathcal{L}}(e^{-iHt'}\rho e^{iHt'})$. As can be seen, for $d = 2$ both $\mathrm{Var}(Q_{qu})$ and $\langle s_{irr}^{qu}\rangle$ monotonically decrease with t. For $d = 3$, however, while $\langle s_{irr}^{qu}\rangle$ monotonically decreases with t, $\mathrm{Var}(Q_{qu})$ does not.

For the qubit case, Fig. 5 puts in perspective the two drastically different energetic footprints of irreversibility in the classical and quantum regime. On the well-known classical side, see Fig. 5a, the average entropy production $\langle s_{irr}^{cl}\rangle$ is equal to the difference between the fixed entropy change ΔS_{cl} associated with the transfer $\eta_{\tilde{\theta}} \to \tau_1$, and an absorbed heat $\langle Q_{cl}\rangle$ when this transfer is achieved by an irreversible thermalization process, divided by the temperature T. The classical heat footprint $\langle Q_{cl}\rangle$ scales as the thermal energy $k_B T$, an energy scale set by the temperature of the bath that thermalizes the qubit. The more nonthermal the initial (diagonal) qubit state $\eta_{\tilde{\theta}}$ is, the more irreversibility will occur during its thermalization. Hence the classical entropy production $\langle s_{irr}^{cl}\rangle$ increases as the classical non-thermality parameter $nonth(\eta_{\tilde{\theta}})$ deviates from 0. Moreover, $\mathrm{Var}(Q_{cl})$ is dissociated from $\langle s_{irr}^{cl}\rangle$, since as $nonth(\eta_{\tilde{\theta}})$ approaches zero from below, $\langle s_{irr}^{cl}\rangle$ becomes vanishingly small, while $\mathrm{Var}(Q_{cl})$ grows larger.

On the quantum side, see Fig. 5b, the average entropy production $\langle s_{irr}^{qu}\rangle$ equals the entropy change $\Delta S_{qu} = k_B(S_{vN}(\eta_{\tilde{\theta}}) - S_{vN}(\rho_{\tilde{\theta}}))$ associated with the decoherence $\rho_{\tilde{\theta}} \to \eta_{\tilde{\theta}}$ and does not link to an absorbed quantum heat $\langle Q_{qu}\rangle$, as this is always zero. However, both $\langle s_{irr}^{qu}\rangle$ and the quantum heat fluctuations $\mathrm{Var}(Q_{qu})$ vanish when $coh(\rho_{\tilde{\theta}}) = 0$, and monotonously increase with $coh(\rho_{\tilde{\theta}})$, showing the implicit link between quantum entropy production and quantum heat for qubits. This behavior differs markedly from the classical counterpart. Finally, we remark that unlike the classical case, the heat footprint does not scale with temperature but with the system energy gap, here $\hbar\omega_1$, an energy scale set by the quantum character of the system rather than the thermodynamics implied by the bath.

Fundamental bounds for work extraction. Finally, we check the validity of the work footprint of entropy production, Eq. (2), in
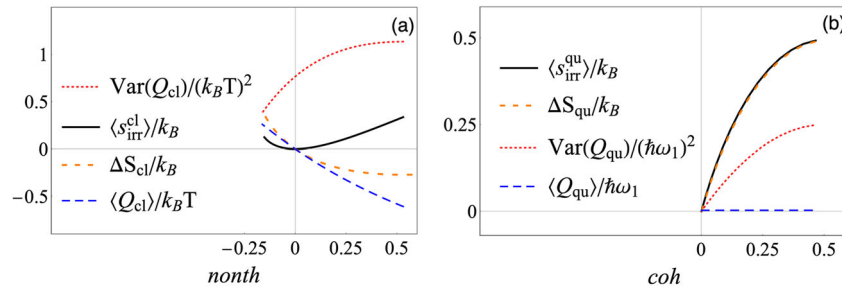
Fig. 5 Heat footprints of irreversibility for a qubit during Step (III). a Positive (negative) non-thermality *nonth* corresponds to a lower (higher) ground state population in $\eta_{\tilde{\theta}}$ than that of the thermal state τ_1. Qubit spacing vs thermal energy ($\hbar\omega_1/k_BT$) is here set such that $q_1 = \langle e_-|\tau_1|e_-\rangle = 0.85$ while $p \in$ [0.5, 1]. Classical entropy production $\langle s_{irr}^{cl}\rangle$ plus the absorbed heat divided by the temperature, $\langle Q_{cl}\rangle/T$, gives the entropy change ΔS_{cl} for any classical non-thermality parameter *nonth*($\eta_{\tilde{\theta}}$). At *nonth* = 0, $\langle s_{irr}^{cl}\rangle = 0$ while the variance in classical heat, Var(Q_{cl}), is strictly positive. Moreover, as *nonth* grows more negative, $\langle s_{irr}^{cl}\rangle$ increases while Var(Q_{cl}) decreases. This demonstrates that the two quantities have no connection. **b** *coh* = 0 implies that $|\tilde{\theta}_\pm\rangle$ are energy eigenstates, while as *coh* → 0.5, $|\tilde{\theta}_\pm\rangle$ become equal superpositions of energy eigenstates. Initial state mixing probability is here set to $p = 0.95$ while $\tilde{\theta} \in [0, \pi/2]$. Quantum entropy production $\langle s_{irr}^{qu}\rangle$ plus zero average quantum heat $\langle Q_{qu}\rangle$ equals the entropy change ΔS_{qu} for any quantum coherence parameter *coh* of initial states $\rho_{\tilde{\theta}}$. Also shown is the quantum heat variance Var(Q_{qu}) in natural units $(\hbar\omega_1)^2$. Both, Var(Q_{qu}) and $\langle s_{irr}^{qu}\rangle$, increase monotonously as *coh* tends to its maximum value of 0.5.

the quantum regime. From the stochastic first law of thermo-dynamics, we observe that for each trajectory Γ of the full pro-tocol (see "Methods" for details) the stochastic extracted work is

$$W_{ext}(\Gamma) = \Delta U^{prot}(\Gamma) + Q_{qu}(\Gamma^q) + Q_{cl}(\Gamma^{cl}) + Q_{cl}^{(IV)}(\Gamma^{(IV)}), \quad (34)$$

where $\Delta U^{prot}(\Gamma) := \mathrm{tr}[H^{(0)}(\Pi[\psi_I] - \Pi[e_{n_N}])]$ is the decrease in internal energy along the trajectory Γ for the full protocol; $Q_{qu}(\Gamma^q)$ and $Q_{cl}(\Gamma^{cl})$ are the quantum and classical heat absorbed during the thermalization process in Step (III); and $Q_{cl}^{(IV)}(\Gamma^{(IV)})$ is the heat absorbed during the quasi-static process of Step (IV). Since $\langle \Delta U^{prot}\rangle = \mathrm{tr}[H^{(0)}(\rho - \eta)] = 0$, while $\langle Q_{qu}\rangle = \mathrm{tr}[H^{(1)}(\tilde{\eta} - \tilde{\rho})] = 0$, the average extracted work reduces to

$$\langle W_{ext}\rangle = \langle Q_{cl}\rangle_{\Gamma^{cl}} + \left\langle Q_{cl}^{(IV)}\right\rangle_{\Gamma^{(IV)}} = -T\langle s_{irr}^{cl}\rangle + T\Delta S_{cl} + T\Delta S^{(IV)}. \quad (35)$$

Here we have assumed quasi-static isothermal trajectories $\Gamma^{(IV)}$ in Step (IV) with $\left\langle s_{irr}^{(IV)}\right\rangle = 0$ and thus

$$\left\langle Q_{cl}^{(IV)}\right\rangle_{\Gamma^{(IV)}} = T\,\Delta S^{(IV)} = T\,k_B(S_{vN}(\eta) - S_{vN}(\tau_1)).$$

Substituting the entropy change across the entire protocol

$$\Delta S^{prot} = \Delta S_{qu} + \Delta S_{cl} + \Delta S^{(IV)},$$

and using $\Delta F^{prot} = -T\Delta S^{prot} = -k_B T(S_{vN}(\eta) - S_{vN}(\rho))$ since $\langle \Delta U^{prot}\rangle = 0$, the result is

$$\langle W_{ext}\rangle = -\Delta F^{prot} - T\left(\langle s_{irr}^{cl}\rangle + \langle s_{irr}^{qu}\rangle\right). \quad (36)$$

Clearly, the optimum work value $-\Delta F^{prot}$ is obtained when neither classical nor quantum entropy production are present and the process is run fully reversibly, as discussed in ref. [27]. Equation (36) now shows how the work is reduced when irreversible steps are included. It is evident that the classical and quantum entropy productions, $\langle s_{irr}^{cl}\rangle$ and $\langle s_{irr}^{qu}\rangle$, limit work extraction in a completely symmetrical manner and when these two contributions are combined Eq. (36) becomes identical to the well-known work footprint of irreversibility, captured by Eq. (2). This footprint is shown in Fig. 6 for the qubit model, where $\langle W_{ext}\rangle$ is plotted as a function of the two parameters that give rise to irreversibility, the quantum coherence *coh* and classical non-thermality *nonth* of the state $\rho_{\tilde{\theta}}$ before thermal contact.

While work extraction is mathematically limited in a symmetrical manner, the physical mechanism is drastically different depending on if the irreversibility of the protocol is of classical or of quantum nature. In the classical regime the irreversibly dissipated heat $\langle Q_{diss}^{sur}\rangle$ is the physical cause of nonoptimal work extraction and exactly compensates the non-recoverable work, i.e., the term $T\langle s_{irr}^{cl}\rangle = \langle Q_{diss}^{sur}\rangle$ in Eq. (36). This energetic footprint of irreversibility equals the average energy change of the qubit during the irreversible thermalization step. But the quantum decoherence step does not give rise to any average energy change—the work extraction is here reduced solely because the system entropy increases, reducing the extracted work by a proportional amount $T\langle s_{irr}^{qu}\rangle = T\Delta S_{qu}$.

To conclude, when a quantum system loses its energetic coherences in a perfectly reversible manner, such as during a quasi-static thermodynamic protocol with a bath at temperature T, the energetic footprint is coherence work[27] while no quantum heat occurs. On the other hand, when a quantum system loses its energetic coherences in a fully irreversible manner, such as during a quantum measurement, the energetic footprint is quantum heat[36] while no coherence work occurs. We here found that when a quantum system loses its energetic coherences in a partially reversible process, see Fig. 1, then the coherence work is in general non-zero, see Fig. 5, albeit reduced from the reversible case by a term proportional to the irreversible (quantum) entropy production, while the quantum heat distribution is also non-zero, see Fig. 3b. Surprisingly, it turned out that these two energetic footprints of irreversibility are not linked through entropy production in the same way as in classical physics.

Discussion

The notion of irreversibility, and how it affects heat and work exchanges, is the core theme of thermodynamics. This paper brings together several strands of recent research in quantum thermodynamics, including stochastic thermodynamics and quantum work extraction protocols, to provide a comprehensive picture of when irreversibility arises in the quantum regime and details the ensuing energetic footprints of irreversibility. Specifically, we have shown that the geometric entropy production as a quantum system in state $\tilde{\rho}$ thermalizes to τ_1, $k_B D[\tilde{\rho}||\tau_1]$, which can be calculated using density matrices, can be understood as arising from the time-reversal asymmetry of quantum stochastic trajectories, Eqs. (17) and (18), in a similar way to classical stochastic thermodynamics. In addition, the quantum eigenstate
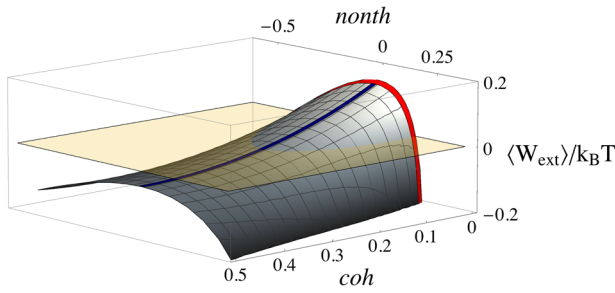
Fig. 6 Average work extraction from a qubit as a function of *coh* and *nonth*. Work (gray) for the full protocol is optimal when neither quantum coherence nor classical non-thermality is present, i.e., *coh* = 0 = *nonth*, and the protocol is run reversibly[27]. $\langle W_{\text{ext}} \rangle$ decreases monotonously with increasing $coh(\rho_{\tilde{\theta}})$ (blue line for *nonth* = 0) and increasing and decreasing $nonth(\rho_{\tilde{\theta}})$ (red line for *coh* = 0). At large deviations from the reversible protocol, $\langle W_{\text{ext}} \rangle$ becomes negative (crosses yellow plane at zero) and work would need to be invested to run the protocol. Parameter choices for initial qubit state ρ_{θ} are $p = 0.8$ and $\theta = \pi/3$.

trajectories allowed for a detailed assessment of work and heat exchanges of a quantum system that can host coherences. While reversible work extraction from quantum coherences has been found[27] to give an "average" work of $\langle W_{\text{ext}} \rangle^{\text{rev}} = -\Delta F^{\text{prot}}$, no distribution of work was provided with respect to which $\langle W_{\text{ext}} \rangle^{\text{rev}}$ is an "average". Here we showed that quantum trajectories naturally give rise to heat as well as work distributions, for which moments, such as the work "average", can be readily calculated. By here including irreversible steps in the work extraction protocol, the reduction of work due to irreversibility has been quantified in Eq. (36). Understanding how imperfect experimental control—which leaves either quantum coherences, or classical non-thermality, or both present in a quantum system before thermal contact—reduces work extraction is important for identifying experimental protocols that are optimal within realistic technical constraints.

While the first moments of heat and work coincide with the values obtained on the density matrix level, the trajectories approach allows access to higher moments. This proved insightful for the discussion of the footprint of quantum irreversibility. We found that the average classical entropy production is linked to the surplus of dissipated heat, see Eq. (23), which is fully analogous to the classical regime, see Eq. (1). Conversely, no such link can be made in regards to quantum entropy production, see Eq. (25). Instead, we show that the quantum entropy production is linked with the fluctuations in quantum heat. Specifically, we show that the average quantum entropy production vanishes if and only if the variance in quantum heat vanishes, while both the average quantum entropy production and the lower bounds to the variance in quantum heat monotonically decrease under Hamiltonian-covariant channels. In the specific case of qubits, we further show that: (i) for a family of states with the same spectrum but different eigenbases, both the fluctuations in quantum heat and the average quantum entropy production monotonically increase with the energy coherence of the eigenbasis; (ii) both the fluctuations in quantum heat and the average quantum entropy production monotonically decrease under the action of Hamiltonian-covariant channels that are a mixture of pure dephasing and depolarization. For higher dimensions, however, this necessary link breaks down in general. We note that a comparable link does not exist in the classical regime where a vanishing classical entropy production is neither necessary nor sufficient for a vanishing variance in classical heat, and even for qubits the two quantities have no monotonic relationship.

It would be interesting to see if the same conclusions hold true when the eigenstate trajectories are replaced by experimentally measured trajectories and their probabilities, for which the analysis presented here can be implemented in an analogous manner. Another open problem is to establish a unique measure of the fluctuations in quantum heat for degenerate states. It is known that if a quantum state has degenerate eigenvalues, then it offers infinitely many eigenstate decompositions, and hence the variance in quantum heat as quantified by Eq. (27) will not be uniquely defined by the quantum state alone. While the lower and upper bounds in Eq. (28) are independent of such an eigenstate decomposition, it would be interesting to introduce an operational procedure for measuring the fluctuations in quantum heat which are independent of the eigenstate decomposition of the system's state.

Methods

In this section we provide detailed technical calculations for our main results, presented in the main text above. First, we describe the eigenstate trajectories for the full work extraction protocol, and the resulting entropy productions; Next we evaluate the variances in quantum and classical heat as a quantum system thermalizes, both for general d-dimensional systems and for qubits; Finally we show that the energy coherence for all qubit states decreases under quantum channels that are a convex combination of dephasing with respect to the energy eigenbasis, and depolarization to the complete mixture.

Trajectories for the full work extraction protocol. We now introduce the full trajectories of the protocol, with expressions for their probabilities, and evaluate the stochastic entropy production associated with each trajectory. We shall show that the full entropy production can be split into entropy production terms associated for each step. Next, we show that the average entropy production for the full protocol reduces to the average entropy production for Step (III) in the limit that the evolution in Step (IV) becomes quasi-static.

Recall that the work extraction protocol can be split as follows. Step (I): unitary evolution $\rho \mapsto \tilde{\rho}$; Step (II): Hamiltonian quench $H^{(0)} \mapsto H^{(1)}$; Step (III): decoherence $\tilde{\rho} \mapsto \tilde{\eta}$ followed by classical thermalization $\tilde{\eta} \mapsto \tau_1$; Step (IV): quasi-static evolution $\tau_1 \cdots \mapsto \tau_N \equiv \eta$; and Step (V): Hamiltonian quench $H^{(N)} \mapsto H^{(0)}$. Since Steps (II) and (V) are only Hamiltonian quenches, and do not alter the state, we shall not include these when constructing our trajectories.

Each thermalization process that the system undertakes is described by the channels $\Lambda_i : \rho \mapsto \text{tr}_{\mathcal{B}_i}[\mathcal{V}_i(\rho \otimes \tau_{\mathcal{B}_i})\mathcal{V}_i^{\dagger}]$, where $\mathcal{B}_1 \equiv \mathcal{B}$ and $\mathcal{V}_1 \equiv \mathcal{V}$ are the bath and unitary used in Step (III), while $\mathcal{B}_2, \dots, \mathcal{B}_N$ and $\mathcal{V}_2, \dots, \mathcal{V}_N$ are the baths and unitaries used in Step (IV). We shall decompose each thermalization channel into their Kraus operators $K_{\mu_i, \nu_i} := \sqrt{\langle \mu_i | \tau_{\mathcal{B}_i} | \mu_i \rangle} \langle \nu_i | \mathcal{V}_i | \mu_i \rangle$, where $|\mu_i\rangle$ and $|\nu_i\rangle$ are eigenstates of bath Hamiltonian $H_{\mathcal{B}_i}$, with energy eigenvalues $\epsilon_{\mu}(i)$ and $\epsilon_{\nu}(i)$, respectively. Such Kraus operators are constructed if, before and after the bath's joint unitary evolution with the system, we subject it to projective energy measurements.

The full trajectory that the system takes during the protocol, therefore, can be expressed as

$$\Gamma = \Gamma_{(l, n_0, \dots, n_N), (\mu_1, \nu_1), (\mu_2, \nu_2), \dots (\mu_N, \nu_N)} , \tag{37}$$

where $\Gamma_{\mathcal{S}} := (l, n_0, \dots, n_N) \equiv |\psi_l\rangle \mapsto |\tilde{\psi}_l\rangle \mapsto |e_{n_0}\rangle \mapsto \cdots \mapsto |e_{n_N}\rangle$ is the sequence of time-local eigenstates of the system during the protocol. Note that, here, we identify $n_0 \equiv m$ and $n_1 \equiv n$ as the eigenstate labels during Step (III). The bath indices (μ_i, ν_i) merely indicate the sequence of energy measurement outcomes on the baths, and they only contribute to the probabilities of the system trajectories $\Gamma_{\mathcal{S}}$. The probability of the trajectory Γ is evaluated to be

$$P(\Gamma) = \langle \tilde{\psi}_l | \tilde{\rho} | \tilde{\psi}_l \rangle \| \mathcal{K}_{\Gamma} \|^2,$$
$$= \langle \tilde{\psi}_l | \tilde{\rho} | \tilde{\psi}_l \rangle \, |\langle \tilde{\psi}_l | e_{n_0} \rangle|^2 \prod_{i=1}^{N} \langle \mu_i | \tau_{\mathcal{B}_i} | \mu_i \rangle \, |\langle e_{n_i} \nu_i | \mathcal{V}_i | e_{n_{i-1}} \mu_i \rangle|^2, \tag{38}$$

where we have introduced the full Kraus operator for the protocol,

$$\mathcal{K}_{\Gamma} := \Pi[e_{n_N}] K_{\mu_N, \nu_N} \cdots \Pi[e_{n_1}] K_{\mu_1, \nu_1} \Pi[e_{n_0}] \Pi[\tilde{\psi}_l], \tag{39}$$

with $\| \mathcal{K}_{\Gamma} \| := \max_{\phi} \sqrt{\langle \phi | \mathcal{K}_{\Gamma}^{\dagger} \mathcal{K}_{\Gamma} | \phi \rangle} = \sqrt{\langle \tilde{\psi}_l | \mathcal{K}_{\Gamma}^{\dagger} \mathcal{K}_{\Gamma} | \tilde{\psi}_l \rangle}$ denoting the operator norm of $\mathcal{K}_{\Gamma}$. Averaging over all the measurement outcomes on the bath, meanwhile, yields the probabilities for the system-only trajectories $\Gamma_{\mathcal{S}}$, given as

$$P(\Gamma_{\mathcal{S}}) = \langle \tilde{\psi}_l | \tilde{\rho} | \tilde{\psi}_l \rangle \, |\langle \tilde{\psi}_l | e_{n_0} \rangle|^2 \prod_{i=1}^{N} \langle e_{n_i} | \tau_i | e_{n_i} \rangle. \tag{40}$$

Note that we may recover the probability for any sub-trajectory of the system by summing over all other indices of Eq. (40). For example, summing over the indices of Steps (I) and (IV), and the classical thermalization of Step (III), the probabilities for the system's quantum decoherence trajectories $\Gamma_{(l,m)}^{\mathrm{q}}$ are obtained as

$$\sum_{n_{i>0}} P(\Gamma_{\mathcal{S}}) = \langle \tilde{\psi}_l | \tilde{\rho} | \tilde{\psi}_l \rangle \, |\langle \tilde{\psi}_l | e_{n_0} \rangle|^2 = P\left(\Gamma_{(l,m)}^{\mathrm{q}}\right). \tag{41}$$

Summing instead over the indices of Steps (I) and (IV), and the quantum decoherence of Step (III), the probabilities for the system's classical thermalization trajectories $\Gamma_{(m,n)}^{\mathrm{cl}}$ are

$$\begin{aligned}
\sum_{l,n_{i>1}} P(\Gamma_{\mathcal{S}}) &= \sum_l \langle \tilde{\psi}_l | \tilde{\rho} | \tilde{\psi}_l \rangle \, |\langle \tilde{\psi}_l | e_{n_0} \rangle|^2 \langle e_{n_1} | \tau_1 | e_{n_1} \rangle, \\
&= \langle e_m | \tilde{\eta} | e_m \rangle \langle e_n | \tau_1 | e_n \rangle = P\left(\Gamma_{(m,n)}^{\mathrm{cl}}\right).
\end{aligned} \tag{42}$$

We may also reconstruct the full density operator for the system, at any point along the trajectory, see Fig. 2, by weighting the pure states by the total trajectory probabilities that include this term. For example, the average state after the decoherence process in Step (III) is indeed

$$\sum_m |e_m\rangle\langle e_m| \sum_{l,n_1,\ldots,n_N} P(\Gamma_{\mathcal{S}}) = \sum_m |e_m\rangle\langle e_m| \, \langle e_m | \tilde{\eta} | e_m \rangle = \tilde{\eta}. \tag{43}$$

The time-reversed trajectories can be defined by reversing the order of the protocol. Here we have Step (IV): quasi-static reversed isothermal jumps $|e_{n_N}\rangle \mapsto \cdots \mapsto |e_{n_1}\rangle$; Step (III) reversed thermalization $|e_{n_1}\rangle \mapsto |e_{n_0}\rangle$ followed by reversed decoherence $|e_{n_0}\rangle \mapsto |\tilde{\psi}_l\rangle$; and Step (I): reversed unitary evolution $|\tilde{\psi}_l\rangle \mapsto |\psi_l\rangle$. Moreover, we shall consider the time-reversed thermalization maps $\Lambda_i^* : \rho \mapsto \mathrm{tr}_B[\mathcal{V}_i^\dagger(\rho \otimes \tau_B)\mathcal{V}_i]$. Note that the only difference between Λ_i and Λ_i^* is that we have applied the time-reversal operation on the unitaries $\mathcal{V}_i$, transforming them to $\mathcal{V}_i^\dagger$. But since the sequence of measurements on the bath during the forward protocol was (μ_i, ν_i), we shall take the time-reversal sequence of these outcomes, namely, (ν_i, μ_i). As such, the corresponding time-reversed Kraus operators for the thermalization channels will be

$$K_{\nu_i,\mu_i}^* := \sqrt{\frac{\langle \nu_i | \tau_{\mathcal{B}_i} | \nu_i \rangle}{\langle \mu_i | \tau_{\mathcal{B}_i} | \mu_i \rangle}} \langle \nu_i | \mathcal{V}_i^\dagger | \nu_i \rangle = \sqrt{\frac{\langle \nu_i | \tau_{\mathcal{B}_i} | \nu_i \rangle}{\langle \mu_i | \tau_{\mathcal{B}_i} | \mu_i \rangle}} K_{\mu_i,\nu_i}^\dagger = \sqrt{\frac{q_{n_{i-1}}^{(i)}}{q_{n_i}^{(i)}}} \, K_{\mu_i,\nu_i}^\dagger,$$

where $q_{n_i}^{(j)} := \langle e_{n_i} | \tau_j | e_{n_i} \rangle$. Here we have used the fact that, given the energy conservation of the thermalization unitary $\mathcal{V}_i$, it follows that

$$\frac{\langle \nu_i | \tau_{\mathcal{B}_i} | \nu_i \rangle}{\langle \mu_i | \tau_{\mathcal{B}_i} | \mu_i \rangle} = e^{(\epsilon_\mu(i) - \epsilon_\nu(i))/k_B T} = e^{(E_{n_i}^{(i)} - E_{n_{i-1}}^{(i)})/k_B T} = \frac{\langle e_{n_{i-1}} | \tau_i | e_{n_{i-1}} \rangle}{\langle e_{n_i} | \tau_i | e_{n_i} \rangle} = \frac{q_{n_{i-1}}^{(i)}}{q_{n_i}^{(i)}}, \tag{44}$$

where $E_{n_i}^{(j)} := \langle e_{n_i} | H^{(j)} | e_{n_i} \rangle$. Finally, the time-reversed trajectories can be denoted as

$$\Gamma^* = \Gamma_{(n_N,\ldots,n_0,l),(\nu_1,\mu_1),(\nu_2,\mu_2),\ldots,(\nu_N,\mu_N)}^*, \tag{45}$$

which occur with the probability

$$P^*(\Gamma^*) = \langle e_{n_N} | \tau_N | e_{n_N} \rangle ||\mathcal{K}_{\Gamma^*}||^2, \tag{46}$$

where we introduce the time-reversed Kraus operators for the full protocol,

$$\mathcal{K}_{\Gamma^*} := \sqrt{\frac{\prod_{i=1}^N q_{n_{i-1}}^{(i)}}{\prod_{i=1}^N q_{n_i}^{(i)}}} \; \mathcal{K}_\Gamma^\dagger. \tag{47}$$

Now we may evaluate the entropy production for the full protocol, which is given by Eqs. (38) and (46) to be

$$\begin{aligned}
s_{\mathrm{irr}}(\Gamma) &:= k_B \log \frac{P(\Gamma)}{P^*(\Gamma^*)} = k_B \log \frac{\langle \tilde{\psi}_l | \tilde{\rho} | \tilde{\psi}_l \rangle ||\mathcal{K}_\Gamma||^2}{\langle e_{n_N} | \tau_N | e_{n_N} \rangle ||\mathcal{K}_{\Gamma^*}||^2} \\
&= k_B \log \frac{\langle \tilde{\psi}_l | \tilde{\rho} | \tilde{\psi}_l \rangle}{\langle e_{n_N} | \tau_N | e_{n_N} \rangle} + k_B \sum_{i=1}^N \log \frac{q_{n_i}^{(i)}}{q_{n_{i-1}}^{(i)}},
\end{aligned} \tag{48}$$

where we have used the fact that $||\mathcal{K}_\Gamma||^2 = ||\mathcal{K}_\Gamma^\dagger||^2$. Note that the entropy production is independent of the bath measurement results. In other words, the entropy production can be purely determined by the system trajectories $\Gamma_{\mathcal{S}}$.

It is trivial to show that this entropy production can be split into the three terms

$$s_{\mathrm{irr}}(\Gamma) = s_{\mathrm{irr}}^{\mathrm{qu}}\left(\Gamma_{(l,m)}^{\mathrm{q}}\right) + s_{\mathrm{irr}}^{\mathrm{cl}}\left(\Gamma_{(m,n)}^{\mathrm{cl}}\right) + s_{\mathrm{irr}}^{\mathrm{cl}}\left(\Gamma^{(\mathrm{IV})}\right), \tag{49}$$

where $s_{\mathrm{irr}}^{\mathrm{qu}}(\Gamma_{(l,m)}^{\mathrm{q}})$ and $s_{\mathrm{irr}}^{\mathrm{cl}}(\Gamma_{(m,n)}^{\mathrm{cl}})$ are defined in Eqs. (15) and (16), respectively, and

$$s_{\mathrm{irr}}^{\mathrm{cl}}\left(\Gamma^{(\mathrm{IV})}\right) := k_B \log \frac{q_{n_1}^{(1)}}{q_{n_N}^{(N)}} + k_B \sum_{i=2}^N \log \frac{q_{n_i}^{(i)}}{q_{n_{i-1}}^{(i)}} = \sum_{i=2}^N k_B \log \frac{q_{n_{i-1}}^{(i-1)}}{q_{n_{i-1}}^{(i)}} \tag{50}$$

is the entropy production of Step (IV).

Since the average entropy production is additive, i.e., $\langle s_{\mathrm{irr}} \rangle_\Gamma = \langle s_{\mathrm{irr}}^{\mathrm{qu}} \rangle + \langle s_{\mathrm{irr}}^{\mathrm{cl}} \rangle + \langle s_{\mathrm{irr}}^{\mathrm{cl}} \rangle_{\Gamma^{(\mathrm{IV})}}$, we will compute each term separately. Let us first turn to the last term, namely, the entropy production in Step (IV). We verify that

averaging over the trajectory probabilities, one obtains

$$\frac{\langle s_{\mathrm{irr}}^{\mathrm{cl}} \rangle_{\Gamma^{(\mathrm{IV})}}}{k_B} = \sum_{i=2}^N \sum_{n_{i-1}} q_{n_{i-1}}^{(i-1)} \log \frac{q_{n_{i-1}}^{(i-1)}}{q_{n_{i-1}}^{(i)}} = \sum_{i=2}^N D[\tau_{i-1} || \tau_i]. \tag{51}$$

When Step (IV) approaches the quasi-static limit, we will have $\sum_{i=2}^N D[\tau_{i-1} || \tau_i] \to 0$, and so $\langle s_{\mathrm{irr}} \rangle_\Gamma = \langle s_{\mathrm{irr}}^{\mathrm{qu}} \rangle + \langle s_{\mathrm{irr}}^{\mathrm{cl}} \rangle$.

Now we turn to the average entropy production during Step (III). Using Eqs. (11) and (15), and introducing the labels $p_l := \langle \tilde{\psi}_l | \tilde{\rho} | \tilde{\psi}_l \rangle$ and $r_m := \langle e_m | \tilde{\eta} | e_m \rangle$, the average quantum entropy production can be shown to be

$$\begin{aligned}
\langle s_{\mathrm{irr}}^{\mathrm{qu}} \rangle &= \sum_{l,m} P\left(\Gamma_{(l,m)}^{\mathrm{q}}\right) \, s_{\mathrm{irr}}^{\mathrm{qu}}\left(\Gamma_{(l,m)}^{\mathrm{q}}\right), \\
&= k_B \sum_{l,m} p_l \, |\langle e_m | \tilde{\psi}_l \rangle|^2 \, \log \frac{p_l}{r_m} = k_B \, D[\tilde{\rho} || \tilde{\eta}],
\end{aligned} \tag{52}$$

as stated in the main text. Here, we used the fact that $\sum_l p_l |\langle e_m | \tilde{\psi}_l \rangle|^2 \log r_m = r_m \log r_m$, and that $\mathrm{tr}[\tilde{\eta} \log \tilde{\eta}] = \mathrm{tr}[\tilde{\rho} \log \tilde{\eta}]$. Meanwhile, the average classical entropy production is given by Eqs. (12) and (16) as

$$\langle s_{\mathrm{irr}}^{\mathrm{cl}} \rangle = \sum_{m,n} P\left(\Gamma_{(m,n)}^{\mathrm{cl}}\right) s_{\mathrm{irr}}^{\mathrm{cl}}\left(\Gamma_{(m,n)}^{\mathrm{cl}}\right) = k_B \sum_m r_m \log \frac{r_m}{q_m} = k_B D[\tilde{\eta} || \tau_1], \tag{53}$$

where here $q_m := \langle e_m | \tau_1 | e_m \rangle$.

Fluctuations in quantum and classical heat. Here, we shall provide expressions for the fluctuations in quantum and classical heat during the thermalization process in Step (III) of the work extraction protocol. For notational simplicity, we shall denote the Hamiltonian as $H = \sum_{m=1}^d E_m \Pi[e_m]$, the initial state of the system as $\rho = \sum_{l=1}^d p_l \Pi[\psi_l]$, its state after decoherence as $\eta := \sum_m r_m \Pi[e_m]$, and its thermal state as $\tau := \sum_n q_n \Pi[e_n]$.

As the system decoheres with respect to the Hamiltonian, we obtain trajectories $\Gamma_{(l,m)}^{\mathrm{q}} := |\psi_l\rangle \mapsto |e_m\rangle$, with probabilities $P(\Gamma_{(l,m)}^{\mathrm{q}}) = p_l |\langle \psi_l | e_m \rangle|^2$ and quantum heat $Q_{\mathrm{qu}}(\Gamma_{(l,m)}^{\mathrm{q}}) := \langle e_m | H | e_m \rangle - \langle \psi_l | H | \psi_l \rangle$. The average quantum heat for a decoherence process is always zero,

$$\langle Q_{\mathrm{qu}} \rangle := \sum_{l,m} P(\Gamma_{(l,m)}^{\mathrm{q}}) \, Q_{\mathrm{qu}}(\Gamma_{(l,m)}^{\mathrm{q}}) = \sum_m \langle e_m | \rho | e_m \rangle \, \langle e_m | H | e_m \rangle - \mathrm{tr}[H \rho] = 0. \tag{54}$$

Hence the variance in quantum heat is equal to its second moment:

$$\begin{aligned}
\mathrm{Var}(Q_{\mathrm{qu}}) &:= \langle Q_{\mathrm{qu}}^2 \rangle - \langle Q_{\mathrm{qu}} \rangle^2 = \langle Q_{\mathrm{qu}}^2 \rangle := \sum_{l,m} P(\Gamma_{(l,m)}^{\mathrm{q}}) \, Q_{\mathrm{qu}}^2(\Gamma_{(l,m)}^{\mathrm{q}}), \\
&= \sum_{l,m} p_l |\langle \psi_l | e_m \rangle|^2 \langle e_m | H^2 | e_m \rangle + \sum_l p_l \langle \psi_l | H | \psi_l \rangle^2 \\
&\quad - 2 \sum_{l,m} p_l |\langle \psi_l | e_m \rangle|^2 \langle \psi_l | H | \psi_l \rangle \langle e_m | H | e_m \rangle.
\end{aligned} \tag{55}$$

Noting that $\sum_m |\langle \psi_l | e_m \rangle|^2 \langle e_m | H^k | e_m \rangle = \langle \psi_l | H^k | \psi_l \rangle$, the variance in quantum heat reduces to

$$\mathrm{Var}(Q_{\mathrm{qu}}) = \sum_l p_l \left(\langle \psi_l | H^2 | \psi_l \rangle - \langle \psi_l | H | \psi_l \rangle^2 \right) = \sum_l p_l \, \Delta(H, \psi_l), \tag{56}$$

where $\Delta(H, \rho) := \mathrm{tr}[H^2 \rho] - \mathrm{tr}[H\rho]^2$ is the variance of the Hamiltonian H in state ρ. In other words, the variance in quantum heat is the average variance of the Hamiltonian in the pure-state components of the initial state ρ.

We now give upper and lower bounds to the variance in quantum heat. For the upper bound we have

$$\Delta(H, \rho) - \mathrm{Var}(Q_{\mathrm{qu}}) = \sum_l p_l \langle \psi_l | H | \psi_l \rangle^2 - \mathrm{tr}[H\rho]^2 = \sum_l p_l \left(\langle \psi_l | H | \psi_l \rangle - \mathrm{tr}[H\rho] \right)^2 \geq 0. \tag{57}$$

To obtain a lower bound, we use the fact that $\Delta(H, \rho) = I_\alpha(H, \rho)$ whenever ρ is a pure state, where $I_\alpha(H, \rho) = \mathrm{tr}[H^2 \rho] - \mathrm{tr}[H\rho^\alpha H \rho^{1-\alpha}]$ for $\alpha \in (0, 1)$ is the Wigner–Yanase–Dyson skew information of the observable H in ρ[76]. Using the Lieb concavity theorem[77] it follows that

$$\mathrm{Var}(Q_{\mathrm{qu}}) = \sum_l p_l \, I_\alpha(H, \psi_l) \geq I_\alpha(H, \rho). \tag{58}$$

Combining Eqs. (57) and (58) shows that the variance in quantum heat obeys

$$\Delta(H, \rho) \geq \mathrm{Var}(Q_{\mathrm{qu}}) \geq I_\alpha(H, \rho), \tag{59}$$

where the equalities are saturated if ρ is pure.

As the system thermalizes, we obtain trajectories $\Gamma_{(m,n)}^{\mathrm{cl}} := |e_m\rangle \mapsto |e_n\rangle$, with probabilities $P(\Gamma_{(m,n)}^{\mathrm{cl}}) = r_m q_n$ and classical heat

$Q_{cl}(\Gamma^{cl}_{(m,n)}) := \langle e_n|H|e_n \rangle - \langle e_m|H|e_m \rangle$. The average classical heat is therefore

$$\langle Q_{cl} \rangle := \sum_{m,n} P(\Gamma^{cl}_{(m,n)}) Q_{cl}(\Gamma^{cl}_{(m,n)}) = \sum_{m,n} r_m q_n \mathrm{tr}[H(\Pi[e_n] - \Pi[e_m])]$$

$$= \mathrm{tr}[H(\tau - \eta)] \equiv \mathrm{tr}[H(\tau - \rho)], \tag{60}$$

while the second moment is

$$\langle Q^2_{cl} \rangle := \sum_{m,n} P(\Gamma^{cl}_{(m,n)}) Q_{cl}(\Gamma^{cl}_{(m,n)})^2,$$

$$= \sum_{m,n} r_m q_n (\mathrm{tr}[H\Pi[e_n]]^2 + \mathrm{tr}[H\Pi[e_m]]^2 - 2\mathrm{tr}[H\Pi[e_n]]\mathrm{tr}[H\Pi[e_m]]),$$

$$= \mathrm{tr}[H^2(\tau + \eta)] - 2\mathrm{tr}[H\tau]\mathrm{tr}[H\eta]$$

$$\equiv \mathrm{tr}[H^2(\tau + \rho)] - 2\mathrm{tr}[H\tau]\mathrm{tr}[H\rho]. \tag{61}$$

Note that here we have used the fact that $\mathrm{tr}[H^k \eta] = \sum_n \mathrm{tr}[H^k \Pi[e_n]\rho\Pi[e_n]] = \mathrm{tr}[H^k \rho]$.

The variance in classical heat, therefore, is

$$\mathrm{Var}(Q_{cl}) := \langle Q^2_{cl} \rangle - \langle Q_{cl} \rangle^2 = \Delta(H, \eta) + \Delta(H, \tau) \equiv \Delta(H, \rho) + \Delta(H, \tau). \tag{62}$$

Quantum and classical heat variances for a qubit. Let us first consider the variance in quantum heat for the decoherence trajectories Γ^q of a qubit in state $\rho_{\hat{\theta}} = p\Pi[\hat{\theta}_-] + (1-p)\Pi[\hat{\theta}_+]$ and with Hamiltonian $H^{(1)} = \frac{\hbar\omega_1}{2}(\Pi[e_+] - \Pi[e_-])$. One finds that when $d = 2$, the matrix elements of the doubly stochastic matrix M (Θ) are $M^{(\Theta)}_{k \neq l, l} = \frac{1}{2}\sin^2(\Theta\pi/2)$, and $M^{(\Theta)}_{l,l} = 1 - \frac{1}{2}\sin^2(\Theta\pi/2)$. By solving the equation $|\tilde{\theta}| = 2\sin^{-1}(\sin(\Theta\pi/2)/\sqrt{2})$, we may equivalently write these as $M^{(\tilde{\theta})}_{k \neq l, l} = \sin^2(\tilde{\theta}/2) \equiv coh$, and $M^{(\tilde{\theta})}_{l,l} = 1 - \sin^2(\tilde{\theta}/2) \equiv 1 - coh$, as defined in Eq. (8). We may therefore rewrite Eq. (31) as

$$\Delta(H^{(1)}, \tilde{\theta}_\pm) = coh \sum_{k \in \pm}(E^{(1)}_k - E^{(1)}_\pm)^2 - coh^2 \left(\sum_{k \in \pm}\left(E^{(1)}_k - E^{(1)}_\pm\right)\right)^2,$$

$$= (\hbar\omega_1)^2 (coh - coh^2) \equiv \frac{(\hbar\omega_1)^2}{4}\sin^2(\tilde{\theta}). \tag{63}$$

In the second line, we have used the fact that for the qubit model, $E^{(1)}_k - E^{(1)}_\pm \in \{0, \pm\hbar\omega_1\}$. Since the variance of the Hamiltonian is the same for both eigenstates of the qubit, it follows that the variance in quantum heat is always

$$\mathrm{Var}(Q_{qu}) = \Delta(H^{(1)}, \tilde{\theta}_\pm) = \frac{(\hbar\omega_1)^2}{4}\sin^2(\tilde{\theta}), \tag{64}$$

which monotonically increases as $|\tilde{\theta}|$ increases from 0 to $\pi/2$.

Let us now consider the variance in classical heat for the thermalization trajectories Γ^{cl}. Note that there are only two trajectories which contribute nonvanishing values of classical heat: $|e_-\rangle \mapsto |e_+\rangle$, with absorbed heat $\hbar\omega_1$, occurring with probability $r_{\hat{\theta}}(1 - q_1)$ with $q_1 \geq 1/2$; and $|e_+\rangle \mapsto |e_-\rangle$, with absorbed heat $-\hbar\omega_1$, occurring with probability $(1 - r_{\hat{\theta}})q_1$. From Eq. (62), we can obtain the simplified expression for the classical heat variance as

$$\mathrm{Var}(Q_{cl}) = \Delta(H^{(1)}, \eta_{\hat{\theta}}) + \Delta(H^{(1)}, \tau_1),$$

$$= (\hbar\omega_1)^2 (r_{\hat{\theta}} - r^2_{\hat{\theta}}) + (\hbar\omega_1)^2(q_1 - q^2_1), \tag{65}$$

where $r_{\hat{\theta}} = q_1 \exp(-nonth(\rho_{\hat{\theta}})) \geq 1/2$ is a function of the non-thermality of the state $\rho_{\hat{\theta}}$. Hence $\mathrm{Var}(Q_{cl})$ monotonously increases with $nonth(\rho_{\hat{\theta}})$, see also Fig. 5.

Hamiltonian-covariant channels and energy coherence for qubits. In order to see how Hamiltonian-covariant channels affect the energy coherence of the eigenbasis of ρ, it will be useful to work in the geometric picture of the Bloch sphere, where $\rho = \frac{1}{2}(1 + \vec{n}\cdot\vec{\sigma})$ and $H = \frac{\hbar\omega}{2}\sigma_3$. Here $\vec{n} := (n_1, n_2, n_3)$ is the Bloch vector such that $n_i \in \mathbb{R}$ and $|\vec{n}| \leq 1$, and $\vec{\sigma} := (\sigma_1, \sigma_2, \sigma_3)$ with σ_i the Pauli matrices. As such, the spectral projections of H and ρ can be expressed as

$$\Pi[e_\pm] := \frac{1}{2}(1 \pm \sigma_3), \qquad \Pi[\theta_\pm] := \frac{1}{2}\left(1 \pm \frac{\vec{n}}{|\vec{n}|}\cdot\vec{\sigma}\right), \tag{66}$$

which give the energy coherence of the eigenbasis of ρ as

$$coh(\rho) := \min_{i,j}\mathrm{tr}[\Pi[e_i]\Pi[\theta_k]] = \frac{1}{2}\left(1 - \frac{|n_3|}{|\vec{n}|}\right). \tag{67}$$

In other words, the energy coherence decreases as the fraction of the Bloch vector along the Hamiltonian axis $x_3 := (0, 0, 1)$ increases, where we note that here, we define $0/0 := \lim_{x \to 0} x/x = 1$, meaning that the energy coherence of the complete mixture is zero. Now let us consider the two states $\rho = \frac{1}{2}(1 + \vec{n}\cdot\vec{\sigma})$ and $\mathcal{E}(\rho) = \frac{1}{2}(1 + \vec{m}\cdot\vec{\sigma})$. We therefore have

$$coh(\rho) - coh(\mathcal{E}(\rho)) = \frac{1}{2}\left(\frac{|m_3|}{|\vec{m}|} - \frac{|n_3|}{|\vec{n}|}\right) \geq 0 \iff \frac{|m_3|^2}{|\vec{m}|^2} \geq \frac{|n_3|^2}{|\vec{n}|^2}. \tag{68}$$

Now we wish to see what subset of Hamiltonian-covariant channels $\mathcal{E}$ will guarantee that $coh(\rho) - coh(\mathcal{E}(\rho)) \geq 0$ for all ρ.

Due to the convex structure of quantum channels[89], any quantum channel that maps from a d-dimensional Hilbert space to itself can be constructed as a convex combination of "extremal" quantum channels $\{\mathcal{E}_i\}$ where extremality of $\mathcal{E}_i$ is defined as $\mathcal{E}_i = \lambda\mathcal{E}_j + (1 - \lambda)\mathcal{E}_k$, with $\lambda \in [0, 1]$, only if $\mathcal{E}_j = \mathcal{E}_k = \mathcal{E}_i$. In the special case of $d = 2$, as shown in Corollary 15 of ref. [90], a quantum channel $\mathcal{E}$ is extremal if either $\mathcal{E}_i$ is unitary, or it is not a convex combination of unitary channels and the rank of its corresponding Choi-state is 2. The Choi-state associated with a qubit quantum channel $\mathcal{E}$ is defined as

$$\rho_\mathcal{E} := (\mathcal{E} \otimes 1)\Pi[\Phi_+], \tag{69}$$

where $|\Phi_+\rangle := \frac{1}{\sqrt{2}}(|\varphi_+, \varphi_+\rangle + |\varphi_-, \varphi_-\rangle)$ with $\{|\varphi_\pm\rangle\}$ any orthonormal basis of $\mathbb{C}^2$. Therefore, we may always write a qubit channel $\mathcal{E}$ as

$$\mathcal{E}(\rho) = \lambda\,\mathcal{U}(\rho) + (1 - \lambda)\mathcal{T}(\rho), \tag{70}$$

where $\lambda \in [0, 1]$ and

$$\mathcal{U}(\rho) = \sum_j p_j\,\mathcal{U}_j(\rho), \qquad \mathcal{T}(\rho) = \sum_k q_k\,\mathcal{T}_k(\rho), \tag{71}$$

with $p_j, q_k > 0$ and $\Sigma_j p_j = \Sigma_k q_k = 1$. Moreover, $\mathcal{U}_j(\rho) := U_j \rho U_j$ with U_j unitary operators, and $\mathcal{T}_k(\rho) = \sum_{l \in \pm} K_{l,k}\rho K^\dagger_{l,k}$, with Kraus operators $K_{+,k} = |\psi_k\rangle\langle\varphi_+|, K_{-,k} = |\psi'_k\rangle\langle\varphi_-|$, where $\{|\psi_k\rangle, |\psi'_k\rangle\}$ are any pair of pure states, not necessarily orthogonal. It is simple to verify, by Eq. (69) and the definition of the Kraus operators above, that $\mathcal{T}_k$ have the Choi states $\rho_{\mathcal{T}_k} = \frac{1}{2}(\Pi[\psi_k, \varphi_+] + \Pi[\psi'_k, \varphi_-])$, which are rank-2 and thus satisfy the extremality condition.

Now let us assume that $\mathcal{E}$ is covariant with respect to the Hamiltonian H, i.e., for any ρ and $t \in \mathbb{R}$, we have $e^{-itH}\mathcal{E}(\rho)e^{itH} = \mathcal{E}(e^{-itH}\rho e^{itH})$. Of course, this means that $\mathcal{U}_j$ and $\mathcal{T}_k$ are also Hamiltonian-covariant, implying that $U_j = e^{i\phi_j\sigma_3}$, so that $\mathcal{U}$ is a probabilistic rotation about the Hamiltonian axis x_3. As for $\mathcal{T}$, let us note that

$$e^{-itH}\mathcal{T}_k(\rho)e^{itH} = \mathcal{T}_k(e^{-itH}\rho e^{itH})$$

$$\Rightarrow e^{-itH}|\psi_k\rangle\langle\psi_k|e^{itH}\langle\varphi_+|\rho|\varphi_+\rangle + e^{-itH}|\psi'_k\rangle\langle\psi'_k|e^{itH}\langle\varphi_-|\rho|\varphi_-\rangle$$

$$= |\psi_k\rangle\langle\psi_k|\langle\varphi_+|e^{-itH}\rho e^{itH}|\varphi_+\rangle + |\psi'_k\rangle\langle\psi'_k|\langle\varphi_-|e^{-itH}\rho e^{itH}|\varphi_-\rangle, \tag{72}$$

implies that $\{|\varphi_\pm\rangle\} \equiv \{|e_\pm\rangle\}$, while $|\psi_k\rangle, |\psi'_k\rangle$ must also be eigenstates of H although, as stated before, they may be the same eigenstate. Therefore, there are only three extremal channels $\mathcal{T}_k$: $\mathcal{T}_1(\rho) = \frac{1}{2}(1 + \sigma_3)$, $\mathcal{T}_2(\rho) = \frac{1}{2}(1 - \sigma_3)$, and $\mathcal{T}_3(\rho) = \frac{1}{2}(1 - n_3\sigma_3)$. Consequently, $\mathcal{T}(\rho) = \frac{1}{2}(1 + v\sigma_3)$, with $v = q_1 - q_2 - q_3 n_3$. It trivially follows that

$$|m_3|^2 = |\mathrm{tr}[\sigma_3\mathcal{E}(\rho)]|^2 = |\lambda\mathrm{tr}[\sigma_3\mathcal{U}(\rho)] + (1 - \lambda)\mathrm{tr}[\sigma_3\mathcal{T}(\rho)]|^2$$

$$= |\lambda n_3 + (1 - \lambda)v|^2 = \lambda^2\beta^2|n_3|^2, \tag{73}$$

where

$$\beta = \left(1 + \frac{1 - \lambda}{\lambda}\frac{v}{n_3}\right). \tag{74}$$

Moreover, denoting $m_\perp = (m_1, m_2, 0)$ as the component of $\vec{m}$ that is orthogonal to x_3, so that $|\vec{m}|^2 = |m_3|^2 + |m_\perp|^2$, and similarly with $n_\perp$, we obtain

$$|m_\perp|^2 = |\mathrm{tr}[(\sigma_1 + i\sigma_2)\mathcal{E}(\rho)]|^2 = \lambda^2|\mathrm{tr}[(\sigma_1 + i\sigma_2)\mathcal{U}(\rho)]|^2 = \delta\lambda^2|\mathrm{tr}[(\sigma_1 + i\sigma_2)\rho]|^2$$

$$= \delta\lambda^2|n_\perp|^2, \tag{75}$$

where $\delta \in [0, 1]$, with $\delta = 1$ if $\mathcal{U}(\rho) = e^{i\phi\sigma_3}\rho e^{-i\phi\sigma_3}$, and $\delta = 0$ when $\mathcal{U}(\rho) = \int_{[0,2\pi]}d\mu(\phi)e^{i\phi\sigma_3}\rho e^{-i\phi\sigma_3} \equiv \sum_{k \in \pm} \Pi[e_k]\rho\Pi[e_k]$ with μ the Haar measure over $[0, 2\pi]$.

As such, we may write

$$\frac{|m_3|^2}{|\vec{m}|^2} = \frac{|m_3|^2}{|m_3|^2 + |m_\perp|^2} = \frac{|m_3|^2}{|m_3|^2 + \delta\lambda^2|n_\perp|^2} = \frac{\beta^2|n_3|^2}{\beta^2|n_3|^2 + \delta|n_\perp|^2}. \tag{76}$$

Consequently, as long as $\beta^2 \geq \delta$, we have

$$\frac{|m_3|^2}{|\vec{m}|^2} \geq \frac{|n_3|^2}{|\vec{n}|^2} \Rightarrow coh(\rho) \geq coh(\mathcal{E}(\rho)). \tag{77}$$

A sufficient condition to ensure that $coh(\rho) \geq coh(\mathcal{E}(\rho))$ for all ρ, irrespective of the value of λ and δ, is if $\mathcal{T}$ is a depolarizing channel, i.e., $\mathcal{T}(\rho) = \frac{1}{2}1$ for all ρ. In this case, $v = 0$ and so $\beta^2 = 1 \geq \delta$.

Code availability
The code used to produce the figures in this article is available from the corresponding author upon reasonable request.

References

1. Goold, J., Huber, M., Riera, A., del Rio, L. & Skrzypczyk, P. The role of quantum information in thermodynamics—a topical review. *J. Phys. A Math. Theor.* **49**, 143001 (2016).
2. Millen, J. & Xuereb, A. Perspective on quantum thermodynamics. *New J. Phys.* **18**, 011002 (2016).
3. Vinjanampathy, S. & Anders, J. Quantum thermodynamics. *Contemp. Phys.* **57**, 545 (2016).
4. Binder, F., Correa, L. A., Gogolin C., Anders J. & Adesso G., eds., *Thermodynamics in the Quantum Regime*, Fundamental Theories of Physics, Vol. 195 (Springer International Publishing, Cham, 2018)
5. Allahverdyan, A. E., Balian, R. & Nieuwenhuizen, T. M. Maximal work extraction from finite quantum systems. *Europhys. Lett.* **67**, 565 (2004).
6. Åberg, J. Truly work-like work extraction via a single-shot analysis. *Nat. Commun.* **4**, 1925 (2013).
7. Frenzel, M. F., Jennings, D. & Rudolph, T. Reexamination of pure qubit work extraction. *Phys. Rev. E* **90**, 052136 (2014).
8. Perarnau-Llobet, M. et al. Extractable work from correlations. *Phys. Rev. X* **5**, 041011 (2015).
9. Skrzypczyk, P., Short, A. J. & Popescu, S. Work extraction and thermodynamics for individual quantum systems. *Nat. Commun.* **5**, 4185 (2014).
10. Lostaglio, M., Korzekwa, K., Jennings, D. & Rudolph, T. Quantum coherence, time-translation symmetry, and thermodynamics. *Phys. Rev. X* **5**, 021001 (2015a).
11. Ćwikliński, P., Studziński, M., Horodecki, M. & Oppenheim, J. Limitations on the evolution of quantum coherences: towards fully quantum second laws of thermodynamics. *Phys. Rev. Lett.* **115**, 210403 (2015).
12. Lostaglio, M., Jennings, D. & Rudolph, T. Thermodynamic resource theories, non-commutativity and maximum entropy principles. *New J. Phys.* **19**, 043008 (2017).
13. Mitchison, M. T., Woods, M. P., Prior, J. & Huber, M. Coherence-assisted single-shot cooling by quantum absorption refrigerators. *New J. Phys.* **17**, 115013 (2015).
14. Korzekwa, K., Lostaglio, M., Oppenheim, J. & Jennings, D. The extraction of work from quantum coherence. *New J. Phys.* **18**, 023045 (2016).
15. Misra, A., Singh, U., Bhattacharya, S. & Pati, A. K. Energy cost of creating quantum coherence. *Phys. Rev. A* **93**, 052335 (2016).
16. Miller, H. J. D. & Anders, J. Time-reversal symmetric work distributions for closed quantum dynamics in the histories framework. *New J. Phys.* **19**, 062001 (2017).
17. Uzdin, R., Levy, A. & Kosloff, R. Quantum heat machines equivalence, work extraction beyond Markovianity, and strong coupling via heat exchangers. *Entropy* **18**, 124 (2016).
18. Ying Ng, N. H., Woods, M. P. & Wehner, S. Surpassing the Carnot efficiency by extracting imperfect work. *New J. Phys.* **19**, 113005 (2017).
19. Streltsov, A., Adesso, G. & Plenio, M. B. Colloquium: quantum coherence as a resource. *Rev. Mod. Phys.* **89**, 041003 (2017).
20. Frenzel, M. F., Jennings, D. & Rudolph, T. Quasi-autonomous quantum thermal machines and quantum to classical energy flow. *New J. Phys.* **18**, 023037 (2016).
21. Klatzow, J. et al. Experimental demonstration of quantum effects in the operation of microscopic heat engines. *Phys. Rev. Lett.* **122**, 110601 (2019).
22. Kwon, H., Jeong, H., Jennings, D., Yadin, B. & Kim, M. S. Clock-work trade-off relation for coherence in quantum thermodynamics. *Phys. Rev. Lett.* **120**, 150602 (2018).
23. Mohammady, M. H. & Anders, J. A quantum Szilard engine without heat from a thermal reservoir. *New J. Phys.* **19**, 113026 (2017).
24. Morikuni, Y., Tajima, H. & Hatano, N. Quantum Jarzynski equality of measurement-based work extraction. *Phys. Rev. E* **95**, 032147 (2017).
25. Uzdin, R. Coherence-induced reversibility and collective operation of quantum heat machines via coherence recycling. *Phys. Rev. Appl.* **6**, 024004 (2016).
26. Uzdin, R., Levy, A. & Kosloff, R. Equivalence of quantum heat machines, and quantum-thermodynamic signatures. *Phys. Rev. X* **5**, 031044 (2015).
27. Kammerlander, P. & Anders, J. Coherence and measurement in quantum thermodynamics. *Sci. Rep.* **6**, 22174 (2016).
28. Solinas, P. & Gasparinetti, S. Probing quantum interference effects in the work distribution. *Phys. Rev. A* **94**, 052103 (2016).
29. Lostaglio, M., Jennings, D. & Rudolph, T. Description of quantum coherence in thermodynamic processes requires constraints beyond free energy. *Nat. Commun.* **6**, 6383 (2015b).
30. del Rio, L., Åberg, J., Renner, R., Dahlsten, O. & Vedral, V. The thermodynamic meaning of negative entropy. *Nature* **474**, 61 (2011).
31. Callens, I., De Roeck, W., Jacobs, T., Maes, C. & Netočný, K. Quantum entropy production as a measure of irreversibility. *Phys D Nonlinear Phenom.* **187**, 383 (2004).
32. Horowitz, J. M. & Parrondo, J. M. R. Entropy production along nonequilibrium quantum jump trajectories. *New J. Phys.* **15**, 085028 (2013).
33. Alonso, J. J., Lutz, E. & Romito, A. Thermodynamics of weakly measured quantum systems. *Phys. Rev. Lett.* **116**, 080403 (2016).
34. Francica, G., Goold, J. & Plastina, F. Role of coherence in the nonequilibrium thermodynamics of quantum systems. *Phys. Rev. E* **99**, 042105 (2019).
35. Santos, J. P., Céleri, L. C., Landi, G. T. & Paternostro, M. The role of quantum coherence in non-equilibrium entropy production. *npj Quantum Inf.* **5**, 23 (2019).
36. Elouard, C., Herrera-Martí, D. A., Clusel, M. & Auffèves, A. The role of quantum measurement in stochastic thermodynamics. *npj Quantum Inf.* **3**, 9 (2017a).
37. Elouard, C., Bernardes, N. K., Carvalho, A. R. R., Santos, M. F. & Auffèves, A. Probing quantum fluctuation theorems in engineered reservoirs. *New J. Phys.* **19**, 103011 (2017b).
38. Manzano, G., Horowitz, J. M. & Parrondo, J. M. R. Quantum fluctuation theorems for arbitrary environments: adiabatic and nonadiabatic entropy production. *Phys. Rev. X* **8**, 031037 (2018a).
39. Manikandan, S. K., Elouard, C. & Jordan, A. N. Fluctuation theorems for continuous quantum measurements and absolute irreversibility. *Phys. Rev. A* **99**, 022117 (2019).
40. Deffner, S. & Lutz, E. Nonequilibrium entropy production for open quantum systems. *Phys. Rev. Lett.* **107**, 140404 (2011).
41. Crooks, G. E. Entropy production fluctuation theorem and the nonequilibrium work relation for free energy differences. *Phys. Rev. E* **60**, 2721 (1999).
42. Seifert, U. Entropy production along a stochastic trajectory and an integral fluctuation theorem. *Phys. Rev. Lett.* **95**, 040602 (2005).
43. Seifert, U. Stochastic thermodynamics, fluctuation theorems and molecular machines. *Rep. Prog. Phys.* **75**, 126001 (2012).
44. Brunelli, M. et al. Experimental determination of irreversible entropy production in out-of-equilibrium mesoscopic quantum systems. *Phys. Rev. Lett.* **121**, 160604 (2018).
45. Ptaszyński, K. & Esposito, M. Thermodynamics of quantum information flows. *Phys. Rev. Lett.* **122**, 150603 (2019).
46. Landau, L. D. & Lifshitz, E. M. *Statistical Physics: Volume 5* (Butterworth-Heinemann, 1980)
47. Balian, R. *From Microphysics to Macrophysics*. (Springer Berlin Heidelberg, Berlin, Heidelberg, 1991).
48. Weinhold, F. *Classical and Geometrical Theory of Chemical and Phase Thermodynamics* (Wiley, 2008) p. 504.
49. Mohammady, M. H. & Romito, A. Conditional work statistics of quantum measurements. *Quantum* **3**, 175 (2019a).
50. Buffoni, L., Solfanelli, A., Verrucchi, P., Cuccoli, A. & Campisi, M. Quantum measurement cooling. *Phys. Rev. Lett.* **122**, 070603 (2019).
51. Elouard, C., Auffèves, A. & Haack, G. Single-shot energetic-based estimator for entanglement in a half-parity measurement setup. *Quantum* **3**, 166 (2019).
52. Anders, J. & Giovannetti, V. Thermodynamics of discrete quantum processes. *New J. Phys.* **15**, 033022 (2013).
53. Gemmer, J. & Anders, J. From single-shot towards general work extraction in a quantum thermodynamic framework. *New J. Phys.* **17**, 085006 (2015).
54. Esposito, M., Lindenberg, K. & Van den Broeck, C. Entropy production as correlation between system and reservoir. *New J. Phys* **12**, 013013 (2010).
55. Manzano, G., Plastina, F. & Zambrini, R. Optimal work extraction and thermodynamics of quantum measurements and correlations. *Phys. Rev. Lett.* **121**, 120602 (2018b).
56. Deffner, S. & Lutz, E. Generalized clausius inequality for nonequilibrium quantum processes. *Phys. Rev. Lett.* **105**, 170402 (2010).
57. Baumgratz, T., Cramer, M. & Plenio, M. Quantifying coherence. *Phys. Rev. Lett.* **113**, 140401 (2014).
58. Marvian, I. & Spekkens, R. W. Extending Noether's theorem by quantifying the asymmetry of quantum states. *Nat. Commun* **5**, 1 (2014).
59. Seifert, U. Stochastic thermodynamics: principles and perspectives. *Eur. Phys. J. B* **64**, 423 (2008).
60. Sekimoto, K. *Stochastic Energetics*, Lecture Notes in Physics, Vol. 799 (Springer Berlin Heidelberg, Berlin, Heidelberg, 2010)
61. Manzano, G., Horowitz, J. M. & Parrondo, J. M. R. Nonequilibrium potential and fluctuation theorems for quantum maps. *Phys. Rev. E* **92**, 032129 (2015).
62. Murashita, Y., Gong, Z., Ashida, Y. & Ueda, M. Fluctuation theorems in feedback-controlled open quantum systems: quantum coherence and absolute irreversibility. *Phys. Rev. A* **96**, 043840 (2017).
63. Grangier, P. & Auffèves, A. What is quantum in quantum randomness? *Philos Trans Royal Soc. A* **376**, 20170322 (2018).
64. Elouard, C. & Mohammady, M. H. Work, Heat and Entropy Production Along Quantum Trajectories, in *Thermodynamics in the quantum regime: Fundamental Aspects and New Directions*, Fundamental Theories of Physics, Vol. 195, (eds Binder, F., Correa, L. A., Gogolin, C., Anders, J. & Adesso, G.) (Springer International Publishing, Cham, 2018) pp. 363–393
65. Haroche, S. & Raimond, J.-M. *Exploring the Quantum* (Oxford University Press, 2006)

66. Gleyzes, S. et al. Quantum jumps of light recording the birth and death of a photon in a cavity. *Nature* **446**, 297 (2007).

67. Campagne-Ibarcq, P. et al. Observing quantum state diffusion by heterodyne detection of fluorescence. *Phys. Rev. X* **6**, 1 (2016).

68. Murch, K. W., Weber, S. J., Macklin, C. & Siddiqi, I. Observing single quantum trajectories of a superconducting quantum bit. *Nature* **502**, 211 (2013).

69. Carmichael, H. J. *Statistical Methods in Quantum Optics 2*, Theoretical and Mathematical Physics (Springer Berlin Heidelberg, Berlin, Heidelberg, 2008)

70. Gammelmark, S. & Mølmer, K. Bayesian parameter inference from continuously monitored quantum systems. *Phys. Rev. A* **87**, 032115 (2013).

71. Perry, C., Ćwikliński, P., Anders, J., Horodecki, M. & Oppenheim, J. A sufficient set of experimentally implementable thermal operations for small systems. *Phys. Rev. X* **8**, 041049 (2018).

72. Lostaglio, M., Alhambra, Á. M. & Perry, C. Elementary thermal operations. *Quantum* **2**, 52 (2018).

73. Huei, N., Ng, Y. & Woods, M. P. *Thermodynamics in the Quantum Regime*, (eds Binder, F., Correa, L. A., Gogolin, C., Anders, J. & Adesso G.), Fundamental Theories of Physics, Vol. 195 (Springer International Publishing, Cham, 2018) pp. 625–650.

74. Ziman, M. & Bužek, V. Open system dynamics of simple collision models, in *Quantum Dynamics and Information* (WORLD SCIENTIFIC, 2010) pp. 199–227.

75. Mohammady, M. & Romito, A. Symmetry constrained decoherence of conditional expectation values. *Universe* **5**, 46 (2019b).

76. Wigner, E. P. & Yanase, M. M. Information contents of distributions. *Proc. Natl Acad. Sci. USA* **49**, 910 (1963).

77. Lieb, E. H. Convex trace functions and the Wigner-Yanase-Dyson conjecture. *Adv. Math.* **11**, 267 (1973).

78. Yanagi, K. Generalized Wigner-Yanase-Dyson skew information and uncertainty relation, in *2010 International Symposium On Information Theory & Its Applications*, Vol. 012015 (IEEE, 2010) pp. 1030–1034

79. Vaccaro, J. A., Anselmi, F., Wiseman, H. M. & Jacobs, K. Tradeoff between extractable mechanical work, accessible entanglement, and ability to act as a reference system, under arbitrary superselection rules. *Phys. Rev. A* **77**, 1 (2008).

80. Ahmadi, M., Jennings, D. & Rudolph, T. The Wigner-Araki-Yanase theorem and the quantum resource theory of asymmetry. *New J. Phys.* **15**, 013057 (2013).

81. Girolami, D. Observable measure of quantum coherence in finite dimensional systems. *Phys. Rev. Lett.* **113**, 1 (2014).

82. Takagi, R. Skew informations from an operational view via resource theory of asymmetry. *Sci. Rep.* **9**, 14562 (2019).

83. Vourdas, A. Quantum systems with finite Hilbert space. *Rep. Prog. Phys* **67**, 267 (2004).

84. Sherman, S. On a conjecture concerning doubly stochastic matrices. *Proc. Am. Math. Soc.* **3**, 511 (1952).

85. Bhatia, R. *Matrix Analysis*, Graduate Texts in Mathematics, Vol. 169 (Springer New York, New York, NY, 1997)

86. Li, Y. & Busch, P. Von Neumann entropy and majorization. *J. Math. Anal. Appl.* **408**, 384 (2013).

87. Ljubenovic, M. Majorization and doubly stochastic operators. *Filomat* **29**, 2087 (2015).

88. Bhatia, R. & Davis, C. A better bound on the variance. *Am. Math. Mon.* **107**, 353 (2000).

89. Heinosaari, T. & Ziman, M. *The Mathematical language of Quantum Theory*. (Cambridge University Press, Cambridge, 2011).

90. Friedland, S. & Loewy, R. On the extreme points of quantum channels. *Linear Algebra Appl.* **498**, 553 (2016).

Author contributions

A.A. and J.A. initiated this study to draw up the connection between the quantum heat[36] and the coherence work[27] for partially reversible processes. M.H.M. derived the skew information bound on the quantum heat variance, (28), and contributed the discussion of the monotonicity of the quantum heat variance for d-dimensional quantum systems. All authors discussed the results and contributed to writing the paper.

Competing interests

The authors declare no competing interests.

Additional information

Supplementary information is available for this paper at https://doi.org/10.1038/s42005-020-0356-9.

Correspondence and requests for materials should be addressed to M.H.M., A.A. or J.A.

Reprints and permission information is available at http://www.nature.com/reprints

Publisher's note Springer Nature remains neutral with regard to jurisdictional claims in published maps and institutional affiliations.